Journal of Geophysical Research: Oceans

RESEARCH ARTICLE
10.1029/2018JC014211

The Biogeochemistry of Electroactive Humic Substances and Its Connection to Iron Chemistry in the North East Atlantic and the Western Mediterranean Sea

Gabriel Dulaquais[1], Matthieu Waeles[1], Loes J. A. Gerringa[2], Rob Middag[2], Micha J. A. Rijkenberg[2], and Ricardo Riso[1]

[1]Laboratoire des Sciences de l'Environnement Marin CNRS UMR 6539, Institut Universitaire Européen de la Mer, Université de Bretagne Occidentale, Plouzané, France, [2]NIOZ Royal Netherlands Institute for Sea Research, Department of Ocean Systems (OCS), Utrecht University, Texel, Netherlands

Key Points:
- First zonal distribution of electroactive humic-like substances (eHS) in the Mediterranean Sea
- In situ production in the euphotic layer and mineralization in the deep sea control eHS distribution
- Probable connection between eHS and iron Mediterranean biogeochemistry through an iron-humic shuttle

Supporting Information:
- Supporting Information S1

Correspondence to:
G. Dulaquais,
gabriel.dulaquais@univ-brest.fr

Citation:
Dulaquais, G., Waeles, M., Gerringa, L. J. A., Middag, R., Rijkenberg, M. J. A., & Riso, R. (2018). The biogeochemistry of electroactive humic substances and its connection to iron chemistry in the North East Atlantic and the Western Mediterranean Sea. *Journal of Geophysical Research: Oceans*, *123*, 5481–5499. https://doi.org/10.1029/2018JC014211

Received 31 MAY 2018
Accepted 11 JUL 2018
Accepted article online 23 JUL 2018
Published online 12 AUG 2018

Abstract We present the zonal distribution of electroactive humic-like substances (eHS) along a section from Offshore Portugal in the North East Atlantic to the Sicily Channel in the Mediterranean Sea. The concentrations were normalized to Suwannee River Fulvic Acid and ranged from 11 μg/L to 81 μg/L. The vertical distributions were typical of those previously reported for dissolved organic carbon in the Mediterranean Sea. High eHS concentrations were measured in surface water and concentrations decreased with depth before increasing again toward benthic maxima measured at some stations. We estimate that eHS represented a relatively small fraction of the natural organic matter in the Mediterranean Sea (2–5%) but considering their important role in the complexation and the solubility of key trace elements (e.g., iron and copper), the eHS cycle could influence the entire biogeochemistry of these marine systems. We identified key processes controlling the concentration of eHS. While biologically mediated production was the major source of eHS, riverine and rain inputs as well as sediment release were also likely external sources. Low eHS concentrations at subsurface depths pointed to photodegradation as a possible sink of eHS, but degradation by heterotrophic bacteria seemed to be the main sink in the deep sea. Finally, we found a positive correlation between dissolved iron and eHS concentrations. Estimation of eHS contribution to iron binding ligand concentrations indicates the complexation of iron by eHS in the Mediterranean Sea. These observations suggest links between the cycles of eHS and iron in the Mediterranean Sea.

1. Introduction

Among the wide range of compounds that make up aquatic dissolved organic carbon (DOC), humic substances account for a substantial part of this pool (up to 20%; Hessen & Tranvik, 2013) with concentrations ranging from tens to hundreds of microgram carbon per liter (Abbt-Braun & Frimmel, 2002; Laglera & van den Berg, 2009; Norman, 2014; Obernosterer & Herndl, 2000; Trimborn et al., 2015). Historically humic substances have been operationally divided between soluble fulvic acids and humic acids. This soil science definition is based on their different solubility in concentrated acid and base solutions (humic acids being insoluble at pH < 1). Here the term "humics" will be used collectively for fulvic and humic acids. Humics can also be distinguished between allochthones humics supplied by river discharge in coastal areas (Alberts & Takács, 1999; Ertel et al., 1986; Waeles et al., 2013) and autochthonous (or marine humics) produced in the ocean interior through microbial processes (Tranvik, 1993). In the aquatic system, the main sink of humics seems to be their photooxidation and subsequent degradation as shown by several studies (Brinkmann et al., 2003; Chen & Bada, 1992; Liu et al., 2010; Mopper et al., 1991). Despite their classification as refractory organic matter, humics may not be so refractory to biological activity. Indeed, studies have shown the biological role of humics in various metabolic pathways such as the positive effect on phytoplankton growth (Prakash & Rashid, 1968) and their key role in the metabolism of nitrogen (Bronk et al., 2007; Müller-Wegener, 1988; See & Bronk, 2005). Direct consumption of humics by bacteria has also been observed (Coates et al., 2002; Cottrell & Kirchman, 2000; Rosenstock et al., 2005).

Another feature of humics is their ability to complex the key trace element iron (Abualhaija et al., 2015; Bundy et al., 2015; Laglera et al., 2011; Laglera & van den Berg, 2009). Iron is recognized as a major regulator of ocean productivity and thus of the ocean's biogeochemistry (Moore et al., 2013; Tagliabue et al., 2017). In marine system, the speciation of dissolved iron (DFe) is dominated by organic complexation >99% (Gledhill & van

den Berg, 1994; Rue & Bruland, 1995). Complexatioof DFe by dissolved organic ligands (L_{Fe}) increases both the solubility and the bioavailability of iron (III); it also decreases the oxidation rate of iron (II) (Boyd & Ellwood, 2010; Liu & Millero, 2002). Organic complexation of iron is thus an important parameter in the marine biogeochemical cycle of this element (Bundy et al., 2015; Gerringa et al., 2015; Gledhill & Buck, 2012; Muller & Cuscov, 2017; Rijkenberg et al., 2008). The exact nature of L_{Fe} is not well defined, nevertheless among the wide range of L_{Fe} (e.g., siderophores, exopolymeric substances, and saccharides), humics have been identified as an important class of L_{Fe} especially in coastal areas and close to shelves (Abualhaija et al., 2015; Laglera & van den Berg, 2009; Mahmood et al., 2015). Because the Mediterranean Sea is surrounded by continents and the main Mediterranean rivers are located in the Western Basin, humics could play an important role in the complexation of DFe in this basin.

In the environment, humics have a "non-constant composition and structure, making it difficult to find an intrinsic 'humic' property that can be used to determine them quantitatively" as stated by Filella (2010). Consequently, the study of humics is dependent of the analytical method used which only allows a partial detection of the entire humic pool. Thanks to the optical properties of humics (Coble, 2007), the zonal and vertical distributions of humic-like fluorescence (HlF) intensities of Chromophoric dissolved organic matter (CDOM) were reported at the basin scale (Coble, 1996; Heller et al., 2013; Jørgensen et al., 2011; Yamashita & Tanoue, 2008, 2009). According to these studies, HlF is relatively weak at the surface, increases with depth and is positively correlated with apparent oxygen utilization (AOU). These observations were interpreted as an "in situ" production of humics by respiration of organic matter, leading to the accumulation of marine humics in the deep sea. However, these methods being more qualitative than quantitative, it can be difficult to interpret the HlF data due to lack of definition of what is really measured (Boyle et al., 2009; Chanudet et al., 2006; Fillela, 2009; Filella, 2010; Penru et al., 2013). Indeed, humics can complex trace elements (e.g., iron and copper) and the quantitative study of humics by fluorescence can be biased by quenching phenomena (Poulin et al., 2014; Yamashita & Jaffé, 2008). Alternatively, electrochemical methods on a mercury drop electrode can be used to analyze humic-like substances (HS) in seawater (Laglera et al., 2007; Pernet-Coudrier et al., 2013; Quentel et al., 1986, 1987). Besides allowing analysis at very low signal levels (μg C/L), these methods provide a quantification of HS that can complex trace metals which will be called electroactive HS (eHS) hereafter. Despite being standard dependent (Quentel & Filella, 2008), these methods are semiquantitative and allow intercomparison in term of concentration between the data sets generated. To date, humic data generated by electrochemical methods are scarce and mostly restricted to the surface layer and to coastal areas (Laglera et al., 2007; Laglera & van den Berg, 2009; Norman, 2014; Slagter et al., 2017; Trimborn et al., 2015), and to our knowledge, there is no eHS data published in the Mediterranean Sea. A recent study (see Figure 2 in Hassler et al., 2017) provides data along the water column (0–1,000 m) acquired at one station in the South Pacific (Tasman Sea) with concentration decreasing from the surface to the deep sea that contrast with the deep enrichment in humic-like fluorescence often recorded. Similarly in the Artic Sea, Slagter et al. (2017) also found a decrease of eHS concentrations from the surface to the mesopelagic waters suggesting a possible mineralization of eHS along the water column.

In this context, we investigated the spatial and vertical distributions of eHS along a zonal section crossing the Eastern part of the temperate Atlantic Ocean and the entire Western Mediterranean Basin (Figure 1). The relatively high vertical and spatial resolution of sampling has allowed a quantitative study of eHS in these two contrasting marine systems. Here we present full-depth vertical profiles of eHS and we identified key processes controlling eHS behavior aided by the hydrographic and biogeochemical data set acquired within the framework of the GEOTRACES A04 section. Furthermore, considering the role of eHS in the complexation of the key trace element iron, we explored the potential connections between the iron and eHS cycles. This study provides a new step in our understanding of the marine biogeochemistry of metal binding ligands.

2. Methods

2.1. Sampling

Samples were collected aboard the Dutch R/V Pelagia at 10 stations along the eastern part of the GEOTRACES-A04N section between 15 and 24 May 2013 (Figure 1). All samples were collected using the TITAN-CTD frame of NIOZ (the Netherlands), with 24 ultraclean sampling PRISTINE bottles of 24 L each made of polyvinylidene fluoride and titanium (Rijkenberg et al., 2015). After deployment the TITAN system was

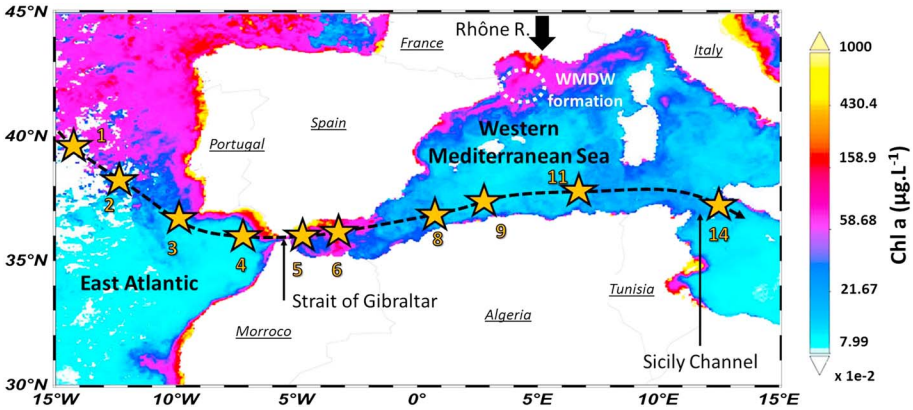

Figure 1. Cruise track of the western part of GEOTRACES A04N, yellow stars indicate sampling station locations. The colors indicate the average chlorophyll *a* concentrations during the period of the cruise (15 to 24 May 2013, generated using Moderate Resolution Imaging Spectroradiometer (MODIS)-AQUA model). The mouth of the river Rhône and the location of western Mediterranean deep water convection are indicated.

moved to a Class-100 container for subsampling (de Baar et al., 2008). Here all samples were collected using inline filtration under N_2 pressure (filtered 99.99% N_2, 0.7 atm). Seawater was then filtered through 0.2-µm Sartobran 300 cartridges (Sartorius). Samples for eHS determination were collected in acid cleaned 250-ml HDPE Nalgene® bottles. Before collection, acid cleaned sample bottles were rinsed five times with sample seawater. Seawater samples for analyses were then acidified at a pH of 2 ± 0.05 using ultrapure® HCl (Merck) within an hour after their collection and stored at dark and ambient temperature before analysis in the shore-based laboratory.

2.2. Determination of Electroactive Humic-Like Substances

In this study, eHS were quantified following the method described in Pernet-Coudrier et al. (2013) previously used for the determination of eHS in estuarine and coastal seawater samples (Marie et al., 2017) that we briefly describe in the following paragraph.

Before analysis, samples were introduced into an acid-cleaned electrochemical glass cell and to limit any risk of contamination, aliquots of seawater samples (15.00 ± 0.01 g) were weighed directly into the cell under a laminar flow bench and analyzed immediately after that the pH was checked with a daily calibrated glass combined electrode (Hanna Hi 1331) attached to a Hanna 931400 pH meter (±0.01 precision, NBS scale) and adjusted to 2.0 ± 0.05 with small amounts of diluted solutions (~1 mol/L) of HCl and/or NaOH when necessary. The data were generated using a three-electrode electrochemical device (Metrohm model 663 VA) connected to a potentiostat/galvanostat µAutolab Type III unit monitored by GPES 4.9 software. The working electrode was a static mercury drop electrode, with a drop size of 0.52 mm^2. An Ag/AgCl (3 mol/L KCl, Suprapur®, Merck) electrode and a carbon glass electrode were used as the reference and the auxiliary electrode, respectively. The method used in this work is a follow-up of Quentel et al. (1986, 1992) and is based on the addition of 200-nM (nanomol per litter) Molybdenum (VI) in the sample. After a deaeration step (600 s, stirring, N_2 99,99%) Mo is chelated by the electroactive HS and forms a Mo (VI)-eHS complex. At a deposition potential of 0.000 V (240 s, stirring) the complex is adsorbed to the SDME and is subsequently reduced into Mo (V)-eHS forming a Mo (V)-eHS-Hg complex. After 5 s of equilibration, the potential was swept into a negative direction (down to −0.600 V) using the differential pulse mode, reducing the Mo (V)-eHS-Hg complex which releases Mo (IV) into the solution and provides a quantifiable cathodic current. Details of the mechanism are described in Quentel and Elleouet (2001). The current acquisition was automatically performed by the GPES software. As there is no commercial standard for oceanic waters, we determined the concentration of electroactive HS by standard additions of Suwannee River Fulvic Acid (SRFA, IHSS, R 1S101F) following the recommendations of Quentel and Filella (2008). For each titration, three standard additions were operated and triplicate analyses for each point were done, producing a 12-point calibration curves. After each standard addition a deaeration step (600-s stirring) was performed. All the curves were linear with a correlation coefficient (r^2) > 0.99 ensuring that any measurement error was mostly due to the standard deviation of the initial

sample measurement rather than to the standard additions. The processing of an analytical scan in ultraviolet (UV) irradiated seawater did not show any quantifiable peak at the eHS potential, ensuring no contamination along the different steps of the analysis. Reproducibility was assessed, by standard additions, from eight analyses of the same natural coastal seawater (Bay of Brest). The mean concentration (mean ± SD) was 387 ± 25 μg eq SRFA/L giving a reproducibility of 6%. Repeatability was calculated as the relative standard deviation of 11 consecutive measurements on a 15-ml sample of natural coastal seawater. Repeatability was about 3%. A limit of detection (LOD) was calculated as recommended (IUPAC, 1978): LOD = 3 × SE, where "SE" is the mean standard error from the 11 consecutive measurements. For a deposition time of 240 s, the LOD was 4 μg/L eq SRFA. All data are provided with standard errors based on the triplicate analysis. The analysis of HS being standar dependent (Quentel & Filella, 2008), we normalized results in microgram per liter of equivalent SRFA. Similar units were previously reported in the literature for the study of humic substances in marine systems (see review by Hassler et al., 2017). Previous study on the effect of glutathione and exopolymeric substances on the eHS signal demonstrated that these substances does not generate any quantifiable peak at the eHS potential (−0.43 V versus Ag/AgCl) ensuring that eHS quantification is not interfered by these compounds (Chanudet et al., 2006).

2.3. Intercomparison With Fe-eHS Method

Most of the recent oceanographic studies of eHS (Bundy et al., 2014; Laglera & van den Berg, 2009; Slagter et al., 2017) were conducted using the method developed by Laglera et al. (2007) and based on the complexation of eHS by dissolved iron at natural pH (called Fe-eHS method hereafter). In order to ensure that eHS data acquired by the method developed by Pernet-Coudrier et al. (2013; called Mo-eHS method hereafter) can be compared to those generated by the Fe-eHS method, we conducted an intercomparison exercise between both methods on eight seawater samples from contrasted marine systems (Figure 2 and Table S1 in the supporting information; North Pacific, North West Atlantic, Mediterranean Sea, and coastal North East Atlantic). Analysis of eHS by the Fe-eHS method were performed at a pH of 8.05 following the analytical procedure describes in Laglera et al. (2007) and adapted with the recommendations of Bundy et al. (2014).

Results of this intercomparison (Figure 2) show excellent agreement between the two methods (Mo-eHS = 1.05 ± 0.09 Fe-eHS + 2.36 ± 5.02 μg/L, $R^2 > 0.99$). The analysis of a Deep Seawater Reference sample (Hansell lab, Batch 2017) in which eHS concentration was determined at 49 ± 3 and at 54 ± 4 μg/L eq SRFA by the Mo-eHS and the Fe-eHS methods respectively exemplified the good agreement between these two electrochemical methods. Slightly higher values were generally obtained with the Mo-method (+5%); however, this difference was within the uncertainties on the measurements (9%). Results of this intercomparison exercise demonstrate that both methods allow a comparable quantification of eHS in seawater.

2.4. Comparison With LC-OCD

Analysis of HS by electrochemical methods is defined by the standard used (Quentel & Filella, 2008); thus, any change in the quality of humic substances along the water column could potentially induce bias of measurement. In order to ensure that variations of eHS concentrations along the water column relies on environmental processes, we analyzed 24 samples from a station in the Mediterranean sector (Station 11) using liquid chromatography with an organic carbon detector equipped with a size exclusion column (SEC-LC-OCD). This method operationally defines a humic substances fraction (Huber et al., 2011) and has been previously used for the determination of humics in marine samples (Dittmar & Kattner, 2003). It allows the quantification of humic substances in terms of carbon concentration, which can be then converted into equivalent SRFA using the carbon content of SRFA (52.44% of C for SRFA 1S101F). Both methods show a very similar vertical distribution (Figure S1) with a maximum concentration in the surface and a minimum in the deep sea. SEC-LC-OCD measurements were significantly higher than eHS concentrations indicating that eHS is a fraction prone to similar biogeochemical processes as the total humic pool. LC-OCD results will be further discussed elsewhere.

2.5. Additional Data Set

Hydrological data sets including chlorophyll *a* used in this study were acquired using a CTD package. As described in Gerringa et al. (2017), it consisted of a SeaBird SBE9 plus underwater unit, a SBE11plusV2 deck unit, an SBE3plus temperature sensor, an SBE4 conductivity sensor, a Wetlabs C-Star transmissometer

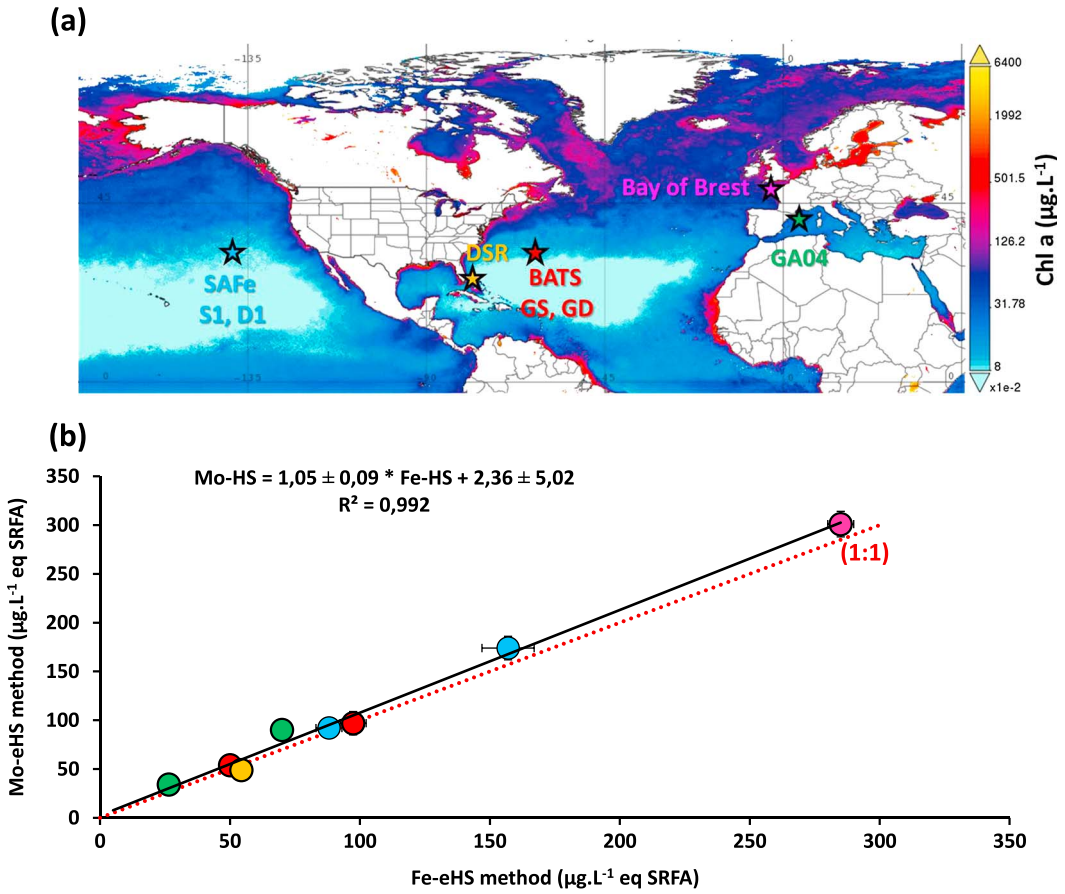

Figure 2. (a) Map of the sampling locations (stars) of the different seawater samples used for the intercomparison exercise for the determination of electroactive humic-like substances. Details of exact locations and depth can be found in Table S1. (b) Scatterplot of the intercomparison exercise between the method developed by Laglera et al. (2007) (Fe-eHS method) and the method developed by Pernet-Coudrier et al. (2013) used in this study (Mo-eHS method). Red dashed line represents the equivalence line. Uncertainties on measurements are indicated and uncertainties on the regression are provided for 95% of confidence interval.

(25 cm, deep, red), and an SBE43 dissolved oxygen sensor. Fluorescence was measured as the beam attenuation coefficient at 660 nm using a Chelsea Aquatracka MKIII fluorometer. The fluorometer signal was calibrated against chlorophyll *a* and is expressed as µg Chl *a*/L. The Practical salinity (PSS-78) and the potential temperature (T-90) were used to derived absolute salinity (S_A in g/kg) and conservative temperature (Θ in °C) using the GSW software version 3.06 for MATLAB (McDougall & Barker, 2011). Apparent utilization of oxygen values (AOU, in mol/kg) were estimated using Ocean Data View software (Schlitzer, 2007) and normalized to mole per liter sing density anomalies (σ_Θ).

The DFe, iron binding ligands (L_{Fe}), and conditional stability constants (K′) data sets used in this study are those published by Gerringa et al. (2017). DFe were generated onboard by flow injection analysis following the method described in Rijkenberg et al. (2014). The analysis of the organic complexation of DFe was executed by competing ligand exchange adsorptive cathodic stripping voltammetry using 2-(2-Thiazolylazo)-p-cresol as competitive ligand (Croot & Johansson, 2000). Using a nonlinear regression of the Langmuir isotherm, the electrical signal recorded in nanoampere was converted into a concentration in nM, and the ligand concentration [Lt] and the binding strength K′ were estimated (Gerringa et al., 2014).

2.6. Statistical Analysis

Univariable and multivariable correlations were systematically analyzed using the Excel® data analysis toolbox. All linear regression equations given in this study are provided with 95% confidence intervals.

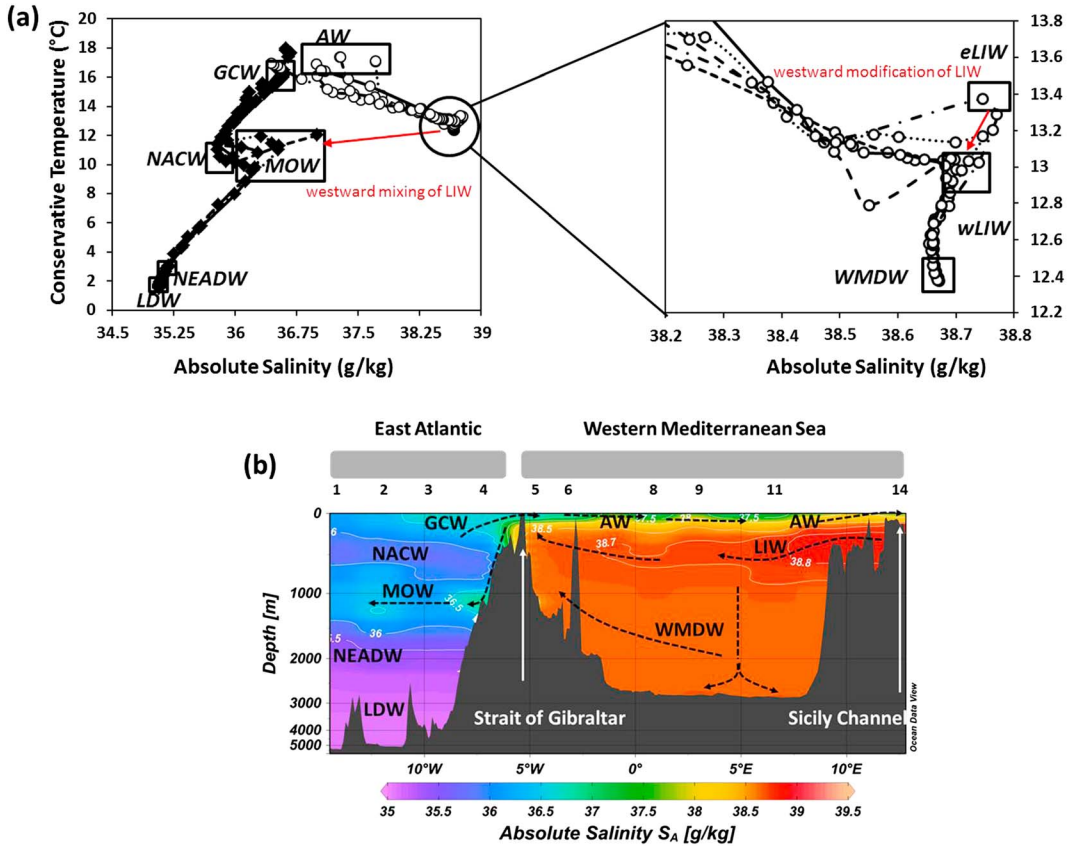

Figure 3. Hydrography of the section in Figure 1. (a) Conservative temperature (Θ)-absolute salinity (S_A) diagram showing the occurrence of Gulf of Cadiz water (GCW), North Atlantic Central Water (NACW), Mediterranean Outflow Water (MOW), North East Atlantic Deep Water (NEADW), Lower Deep Water (LDW), Atlantic Water (AW), Eastern and Western Levantine Intermediate Water (eLIW and wLIW) and Western Mediterranean Deep Water (WMDW) along the section. (b) S_A section generated by ocean data view (Schlitzer, 2007) and simplified circulation. Arrows indicate westward or eastward current respectively. Station numbers are indicated.

In this study we estimated the contribution of the oxidation of eHS to AOU. However, the determination of the contribution of the oxidation of eHS to AOU can be largely biased by simple regression models (e.g., eHS versus AOU) that do not take into account horizontal mixing (Carlson et al., 2010; Takahashi et al., 1985). Moreover, in cases of more than two water masses with unknown chemical properties/end-members, a multiple regression analysis must be done for an accurate determination of organic matter oxidation contribution to AOU (Carlson et al., 2010). In this context we adjusted the eHS-AOU correlations using a multiple linear regression model (1).

$$\mathrm{eHS} = \alpha_1 + \alpha_2 S_A + \alpha_3 \Theta + \alpha_4\ \mathrm{AOU} \tag{1}$$

where α_1, α_2, and α_3 quantify the mixing of the three end-member eHS, absolute salinity (S_A), conservative temperature (Θ), and α_4 is the contribution of the eHS oxidation to AOU. The advantage of this type of model over is that it requires no knowledge of the end-member values for each variable. See Carlson et al. (2010), Li and Peng (2002), and Schneider et al. (2005) for further details of this approach.

3. General Hydrography

The section started from offshore Portugal in the Atlantic, passed through the Strait of Gibraltar, and followed a southern route in the Western Mediterranean Basin up to the Sicily Channel (Figure 1). The general hydrography and biogeochemistry of these areas are described in great detail in Béthoux et al. (1998), Millot and Taupier-Letage (2005), Rolison et al. (2015), and in van Aken (2000a, 2000b). In the next paragraph we briefly describe the general hydrography (Figure 3a) and circulation (Figure 3b).

In the Atlantic Sector, the North Atlantic Central Water was present between 100 and 750 meters (Figures 3a and 3b). This water mass flowing northward across the Eastern Atlantic has a lower salinity (Figure 3a) than the underlying Mediterranean outflow water (MOW, Figure 3a) centered at 1,250 m (Figure 3b). At these latitudes MOW flows westward and entrains the Antarctic Intermediate Waters across the Atlantic Ocean (van Aken, 2000b). Below the MOW, the North Eastern Atlantic Deep Water that follows a southward pathway was recorded. Finally, the lower deep water (Figure 3a), partially composed of Antarctic Bottom Water, follows a northward pathway and occupies the deep zone (>2,500 m). Eastward the section crosses the Strait of Gibraltar that can be simply described as a two-layer system (Figure 3c). There the surface Atlantic Water (AW) enters the Western Mediterranean Basin in the top 160 m, whereas the MOW outflow occurs below 160-m depth (Bryden & Kinder, 1991). Inflowing AW is a mix of North Atlantic Central Water, North Atlantic Surface Water and of the shelf and river influenced waters from the Gulf of Cadiz (Elbaz-Poulichet et al., 2001). MOW mainly consists of modified Levantine Intermediate Water (LIW) slightly mixed with Western Deep Mediterranean Water (Millot & Taupier-Letage, 2005). Going past the Strait of Gibraltar, the section enters the Western Mediterranean Basin (Figure 1).

The surface circulation of the Western basin is mainly driven by circulation of the AW along the continental slopes in a counterclockwise direction. During its advection AW is modified by evaporation increasing its salinity (Figure 3b). The surface Mediterranean Sea is highly stratified from spring to late fall, and the residence time of surface water is on the time scale of a decade (MerMex group, 2011) resulting in limited hydrographic exchange between surface and deeper waters with the exception of areas where LIW and deep water are formed. Nevertheless, intense upwelling cells in the south Western Mediterranean basin can also induce exchange of chemical species between LIW and the surface AW (Millot, 1987). During our expedition the intermediate layer mainly consisted of LIW (Figure 3b). LIW are formed in the Mediterranean Eastern Basin and only penetrates into the Western Basin through the Sicily Channel (Figure 3b) at largest depths. Then, LIW follows the continental slope (Millot & Taupier-Letage, 2005). Along its pathway, LIW is modified (Figure 3a) with surface and deep waters by mesoscale instabilities and finally flows out at the Strait of Gibraltar (Figure 3b). Waters below 2,000 m were mainly composed of Western Mediterranean Deep Water (WMDW, Figures 3a and 3b), a water mass formed on the shelf of the Gulf of Lion (Durrieu de Madron et al., 2013, Figure 1).

4. Results and Discussions

4.1. Vertical and Spatial Distribution of eHS

The concentrations of eHS vary from 11 to 81 μg/L (Figure 4). The lowest concentration was detected in the Mediterranean Sea, at 1,500-m depth at station nine and the highest concentration was recorded at the bottom of the mixed layer at station 1, at 23-m depth. Overall, the vertical distribution of eHS showed similar trends at all stations (Figure 4). With the exception of station 3, all stations had eHS concentrations >40 μg/L in the upper 100–200 m and the highest local eHS concentrations (>50 μg/L) were generally associated with the depth of the Chlorophyll *a* (Chl *a*) maximum (Figures 4 and 5). Low subsurface (10-m depth) concentrations were also observed at several stations (Figure 5). Below the surface mixed layer, eHS decreased with depth while AOU increases (Figures 4 and 5), to concentrations equal to or lower than 25 μg/L in the intermediate layer. Concentrations between 200 and 600 m were similar on both sides of the Strait of Gibraltar, ranging from 18 to 38 μg/L in the Atlantic Ocean and from 16 to 34 μg/L in the Mediterranean Sea (Figure 4). Despite slightly higher concentrations in the Atlantic Ocean (mean $[eHS]_{200–600m\text{-}Atlantic} = 27 \pm 5$; $[eHS]_{200\text{-}600m\text{-}Med\ Sea} = 24 \pm 6$), there were no significant differences on both sides of the Strait of Gibraltar, in contrast to the vertical distribution of eHS differed between the Atlantic Ocean and the Mediterranean Sea. While in the Atlantic eHS concentrations were quasi-uniform between 600- and 4,000-m depth, in the Mediterranean sector eHS kept decreasing with depth down to 11 μg/L (Figure 4). As a result, the Strait of Gibraltar marked a border between the relative young deep HS-depleted Mediterranean water ($[eHS]_{>600m} = 16 \pm 4$ μg/L $n = 34$) and the relatively old HS-rich deep Atlantic water ($[eHS]_{>600m} = 25 \pm 5$ μg/L $n = 33$). Nevertheless, low eHS concentrations were recorded in the deep offshore Atlantic at depths influenced by the MOW ($[eHS]_{MOW} < 20$ μg/L, Figure 4). This water mass was responsible for the lowest eHS concentration recorded in the Atlantic sector (14 μg/L), which occurred at station 2, 1,250-m depth. According to the pathway of the MOW, as identified by its signature salinity (Figure 4b), one would have anticipated the lowest eHS concentration to occur at the maximum depth at station 4.

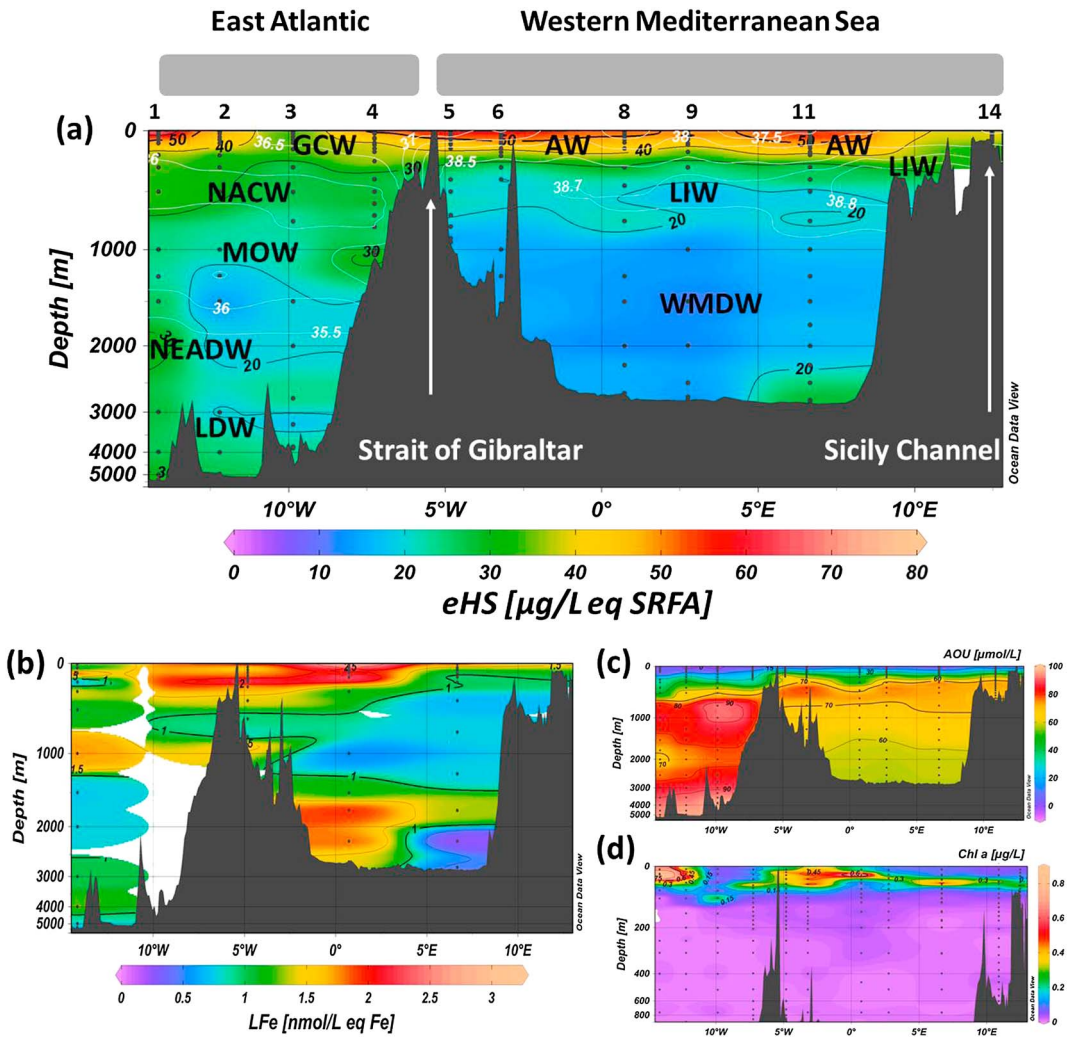

Figure 4. Spatial and vertical distributions along the section of (a) electroactive humic-like substances (eHS), (b) iron binding ligands (L_{Fe}, in equivalent Fe) plotted after Gerringa et al. (2017), (c) apparent utilization of oxygen (AOU, normalized with potential density), and (d) chlorophyll a derived from fluorescence (Chl *a*), note the different vertical scale. White contours in panel (a) indicate absolute salinity (S_A) values. Figures generated using ocean data view (Schlitzer, 2007). GCW = Gulf of Cadiz water; NACW = North Atlantic Central Water; MOW = Mediterranean Outflow Water; NEADW = North East Atlantic Deep Water; LDW = Lower Deep Water; AW = Atlantic Water; WMDW = Western Mediterranean Deep Water; SRFA = Suwannee River Fulvic Acid.

Instead, high HS concentrations (>30 µg/L) were recorded but these probably resulted from a benthic source of eHS rather than to a Mediterranean eHS signature. Indeed, slight to substantial enrichments were observed near the seafloor at some stations along the section (Figure 4). These enrichments were particularly marked at station 4 on the west side of the Strait of Gibraltar and at station 11 in the middle of the South Western Basin. Sediment resuspension induced by seafloor circulation, as suggested by enhanced attenuation coefficient at bottom depth of these two stations (see Figure 2f in Gerringa et al., 2017), benthic microbial production of eHS or release by degradation of organic rich sediments can all be invoked to explain these bottom increases. Although it was identified as a source, our data set did not allow a fine identification of the processes controlling this benthic eHS release and this source is not further discussed in the manuscript.

In the Western Mediterranean Sea, DOC is significantly enriched at the surface with concentrations between 70 and 60 µmol C/L decreasing along the oxycline to a quasi-uniform concentration of 35–40 µmol C/L in the bathypelagic layer (Santinelli et al., 2002, 2010). Moreover, slight DOC enrichments close to the sediments have often been recorded, resulting in a very similar profile between DOC and eHS in the Mediterranean

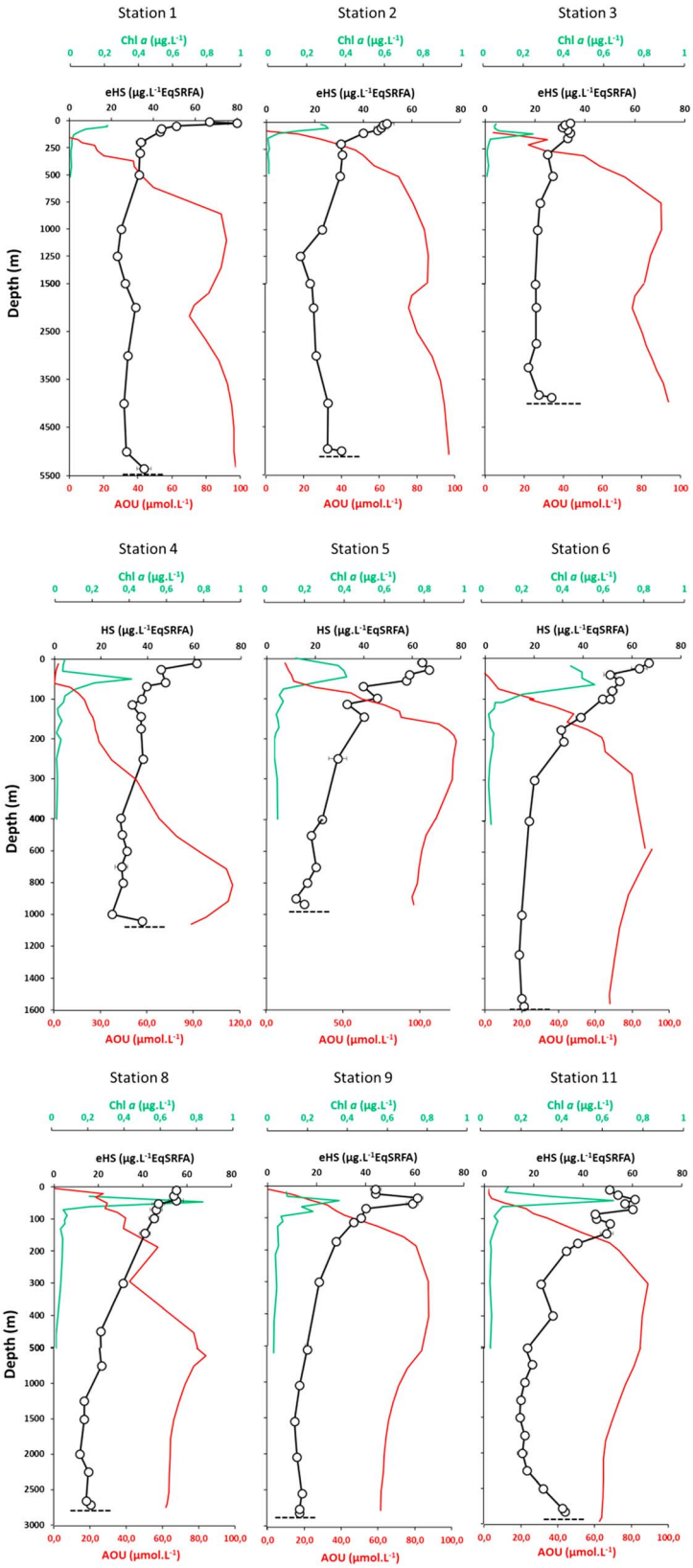

Figure 5. Vertical distribution of electroactive humic like substances (eHS, open black circle; standard deviation is given and falls mostly within the size of the symbol), chlorophyll *a* (Chl *a*, green line), and apparent oxygen utilization (red line). Note the scale changes breaks in the depth axis and the scale difference in apparent oxygen utilization at station 4.

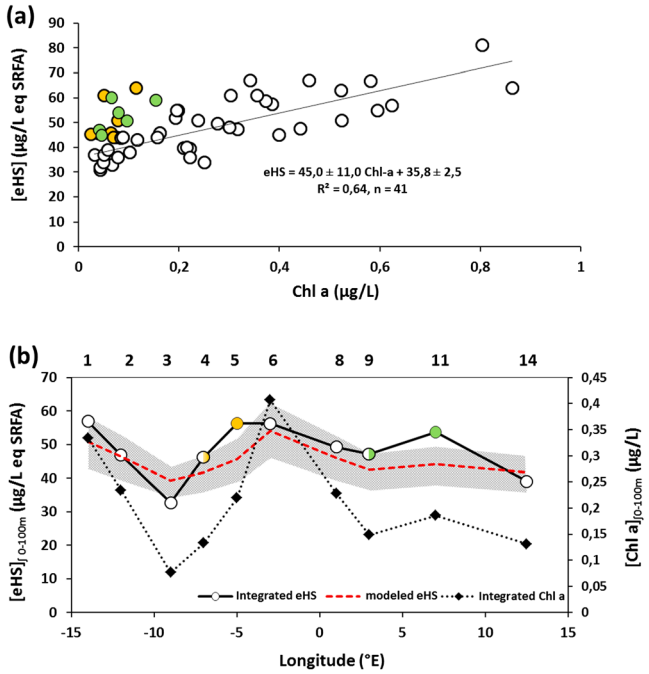

Figure 6. (a) Correlation between electroactive humic-like substances (eHS) and chlorophyll *a* (Chl *a*) in the upper 100 m depth along the section. Colored dots were removed from the regression due to the potential influence of a rain event (green dots, station 11 and 9) and shelf input (yellow dots, station 5 and 4); see text. (b) Calculation of the integrated eHS concentration (red line, left axis) and associated standard error based on the eHS-Chl *a* correlation (gray area) and of integrated Chl *a* concentrations (dark diamonds, right axis). Integrated measured eHS concentrations are indicated (circles). Significant anomalies exist close to Gibraltar (yellow dots) and during the rain event (green dots). Station numbers are given above the figure.

Sea. In order to estimate the contribution of eHS to the Mediterranean DOC pool, we converted the mass concentration into molar concentration of carbon using the percentage of carbon in the SRFA standard we used (52.44% of C for SRFA 1S101F). Based on this conversion and on DOC data determined on samples from this expedition (Mercadante et al., 2016; C. Santinelli, personal communication December 14, 2017), we estimated that only ~ 5% of total Mediterranean DOC is present as eHS in the surface layer and 2 to 4% in the intermediate and deep sea. Despite caveats resulting from the (semi quantitative) method we used, these estimations are in the same range as those previously reported for Open Ocean (Laglera & van den Berg, 2009) and reveal a relatively small contribution of eHS to the total DOC load and distribution. Our estimation is also in good agreement with Penru et al. (2013) which showed, in their study of surface Western Mediterranean seawater, that only 6% of the DOC load is retained by a XAD-8 resin, which is the method adopted by the International Humic Substance Society to isolate humic substances from natural waters.

The vertical distribution of eHS in the Atlantic Ocean and the Mediterranean Sea (Figure 4) displayed opposite trends to what was previously observed for CDOM in other open ocean domains. The vertical profile of humic-like fluorescence generally presents an increase of fluorescence from subsurface to middepth and relatively uniform fluorescence intensities in the deep waters (Catalá et al., 2016; Heller et al., 2013; Yamashita et al., 2010). Our observations are even more surprising since we do not observe strong surface depletion related to photodegradation, whereas the Mediterranean Sea receives high UV incidence all year long. Coastal inputs as well as a significant biological production of eHS in the surface of the Mediterranean Sea (see section 4.2) may compensate eHS loss by photodegradation along the section. These different distributions could also be explained by quenching phenomena. The complexation of iron and copper by humics is known to significantly decrease humic-like fluorescence (Chen et al., 2013; Poulin et al., 2014; Yamashita & Jaffé, 2008) thus involvement of eHS as iron binding ligand (L_{Fe}, see section 4.4) would create an apparent low fluorescence even in the presence of relatively high concentrations. The concomitant high eHS, L_{Fe} (Figures 4a and 4b) and DFe (Gerringa et al., 2017) concentrations in surface waters of the Mediterranean Sea support the hypothesis of fluorescent quenching in this basin. However quenching cannot be invoked for the East Atlantic where high eHS concentrations (Figure 4a) and both low DFe and L_{Fe} concentrations (Figure 4b) were measured. This difference in the vertical distributions of eHS and humic-like fluorescence can also be attributed to a change in the nature of humic with depth. Each analytical method only "sees" a specific fraction of humic substances (Filella, 2010) and the combination of both distributions can be interpreted as a shift in the quality of humic substances from electroactive and poorly fluorescent compounds in surface to less electroactive and highly fluorescent compounds in the deep sea. Further work is needed to confirm (or not) this hypothesis.

4.2. Surface Biogeochemisty of eHS

Photo oxidation of humic substances and the subsequent transformation into labile dissolved organic matter (LDOM) is well documented and known to be a major sink of humic substances in aquatic systems (Brinkmann et al., 2003; Chen & Bada, 1992; Liu et al., 2010; Mopper et al., 1991; Stedmon & Markager, 2005). This sink was depicted by low subsurface (10-m depth) eHS concentrations at some stations along the section (Figure 5). An unexpected feature we recorded is the weak but significant correlation between eHS and Chl *a* (Figure 6a) in the upper 100 m (r^2 = 0.37, n = 55, p value $<$ 0.05). Moreover, when data from stations 9 and 11 and from 4 and 5 were removed from the statistical analysis, the eHS-Chl *a* correlation was markedly improved (r^2 = 0.6, n = 41, p value $<$0.05; ΔeHS/ΔChl *a* = 45 ± 11 at 95% of confidence, Figure 6a). These data were not taken into account due to the probable influence of the Spanish shelf system (stations 4 and 5) and of a severe rain event (stations 9 and 11, Figure S2a) during sampling at these locations

as discussed below. The correlation suggests a positive biological effect on the production of eHS and indicates that a significant part of eHS was produced "in situ." The positive intercept of the regression (Figure 6a) also indicates that part of the eHS pool was produced either before the sampling or had an allochthone origin (riverine, rain or shelf). While active production and excretion of eHS by photosynthetic organisms is unlikely, these biogenic eHS may have been indirectly produced by LDOM transformation by microbial metabolism (Shimotori et al., 2009; Tranvik, 1998) or by its photooxidation following the mechanism proposed by Kieber et al., 1997. Photooxidation requires a time scale of several days (Kieber et al., 1997), whereas LDOM is rapidly (turnover of minutes to day) consumed and/or transformed by heterotrophic bacteria, archea, and also photoautotroph species. Hence, LDOM might not spend enough time in surface waters to allow its conversion in eHS by photooxidation. As a result, the abiotic eHS production is perhaps less intense than the biotic pathway.

Using the Chl *a*-eHS correlation (Figure 6a) and integrated Chl *a* concentrations, we calculated the surface integrated (0–100 m) eHS concentrations (Figure 6b, dashed red line) along the section. When compared to direct observations (Figure 6b, dots), this calculation allows identifying locations where the measured data drift from the Chl *a*-eHS regression, indicating where additional abiotic processes may have impacted the HS surface cycle. A slight negative anomaly of concentration was estimated at station 3, and two positive anomalies were estimated around station 5 and 11. The negative eHS anomaly in the Atlantic can be associated to the photo degradation of eHS resulting from an intense UV irradiation period that occurred during the weeks preceding sampling of station 3 compared to other sampling locations (UV index $>$8; determined after OMI satellite data, https://giovanni.gsfc.nasa.gov). The positive anomalies could be related to two distinct external eHS inputs: (i) riverine discharge combined to lateral transport in the Gibraltar area (station 5) and (ii) a rain event during sampling in the south Western Mediterranean basin (station 11).

At station 5 and to a lesser extent at station 4, eHS concentrations are larger than the calculated concentrations from the regression (Figure 6b). In this sector, surface waters are mainly composed of the inflowing Atlantic waters resulting from the surface circulation at the Strait of Gibraltar. As previously shown for trace elements (e.g., Zn, Cu, Cd, and Co), the chemical composition of this water mass is significantly modified by the surface waters of the Gulf of Cadiz (~20%, Dulaquais et al., 2017; Elbaz-Poulichet et al., 2001; Morley et al., 1997; van Geen et al., 1991), which are influenced by south western Spanish rivers and the shelf. Hence, the enhanced eHS concentrations recorded around station 5 may arise from the Cadiz shelf/river system and have a terrestrial origin. It is well documented that the south western Spanish shelf has a high DOC signature which persists down to the oceanic domain (Dafner et al., 2001). This high DOC load is caused by the riverine discharge of the Guadalquivir River and to a lesser extent Guadalete and Tinto-Odiel rivers. Ribas-Ribas et al. (2011) showed that a substantial amount of the high DOC concentrations they recorded during midspring over the Cadiz Shelf was of terrestrial origin. Moreover, based on the carbon to nitrogen ratio, they related this terrestrial DOC to humic substances. Here everything suggests that Spanish River discharge, combined to the surface circulation in the Gulf of Cadiz, provided a substantial amount of terrestrial eHS to the surface Western Mediterranean Sea.

At station 11, the integrated measured eHS concentration of 53 ± 1 μg/L was significantly higher than the 46 ± 3 μg/L concentrations calculated with the Chl *a*-eHS correlation. This excess of eHS was associated to a rain event that occurred over the week preceding sampling in the surrounding areas of this station (Figure S2a). This rain event was combined with an anticyclonic eddy (Figure S3a), which induced a significant downwelling of 50 m of the surface waters as evidenced by density isolines (Figures S3b) and salinity distributions (Figure S2b) in this area. Moreover, this rain event induced a substantial decrease in salinity in the upper 50 m ($\Delta S_{AJ50m} = 0.43$, Figure S2b) at the time of sampling. Due to the dynamic AW circulation, it would be hard to estimate eHS concentration in rainwater from the rain amounts accumulated at a fixed point. Thus, we used the integrated salt balance to determine the dilution factor between stations 11 and 9 and found 0.989. In the absence of riverine influence, 550 L/m^2 of rainwater were necessary to induce such decrease of salinity over the upper 50 m (Figure S2b). This value is elevated considering the rain event with maximum precipitation of 223 L/m^2; however, the water mass could have followed the rain event resulting in an accumulation of fresh water during its advection before sampling.

The analysis of air mass backward trajectories (Figure S2c) clearly showed that the air mass had been influenced by Western Europe including the Landes Forest (SW France). Because HS can account for a significant

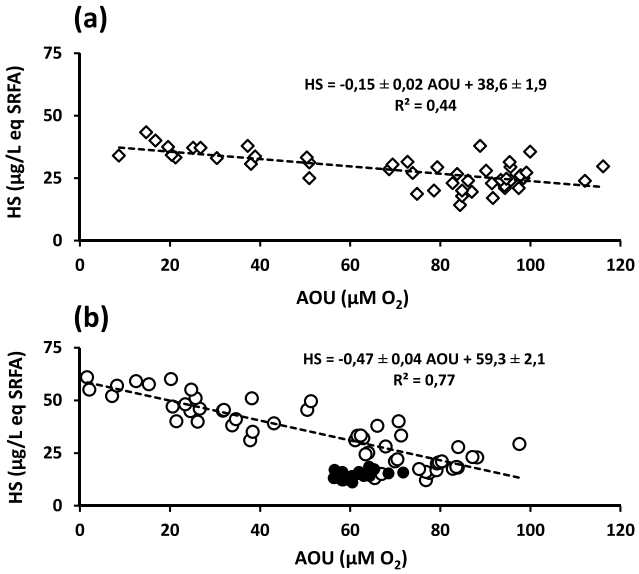

Figure 7. Correlations of the concentration of electroactive humic-like substances (eHS) versus apparent oxygen utilization (AOU) in (a) the Atlantic sector, (b) the Mediterranean sector. In (b) Western Mediterranean Deep Waters data (black dots) were removed from the regression.

pool of the water soluble organic carbon in European aerosols (Paglione et al., 2014; Pavlovic & Hopke, 2012; Salma et al., 2010), the positive eHS anomaly measured at station 11 could be explained by the transfer of eHS-rich water soluble aerosols to the surface water by rain. The eHS rainwater concentration can be estimated by combining the positive integrated eHS anomaly of 0.35 ± 0.15 g/m^2 to the rainwater cumulated volume estimated above. It results in an eHS concentration of 640 ± 250 µg/L. This concentration would be equivalent to an eHS contribution of 28 ± 12 µmol C/L to the DOC load in rainwater. Rainwater DOC load is very variable but concentrations generally vary from 20 to 120 µmol C/L (Kieber et al., 2002; Willey et al., 2000). Humics are thought to be a significant component of the rainwater DOC (Avery et al., 2003; Santos et al., 2009) and account between 20% and 60% of the water soluble organic carbon of European aerosols (Krivácsy et al., 2001; Zappoli et al., 1999); hence, our estimation of the eHS concentration in rainwater is in agreement with rainwater studies.

4.3. Degradation of eHS in Mesopelagic Waters

Humics are often described as refractory organic matter in the literature (Aiken, 1985, Hansell & Carlson, 2014). Their biological production in the surface layer through the microbial carbon pump (Jiao et al., 2010; Shimotori et al., 2009) combined to their sequestration in the ocean interior by oceanic circulation could be a carbon sink. Assuming this is the case, eHS concentrations should increase with depth and would be accumulated in the deep sea with the aging of the water masses as suggested by the increase of HIF CDOM with AOU in the deep Atlantic and Pacific Ocean (Jørgensen et al., 2011; Yamashita & Tanoue, 2008, 2009). A major finding in this study is the absence of eHS increase with depth. On the contrary, eHS decreased with depth with a concomitant increase of AOU in both the Atlantic Ocean and Mediterranean Sea (Figures 4 and 5). In contrast to previous studies, our results suggest a degradation of eHS, especially in the Mediterranean sector, by bacterial respiration. The degradation of eHS with aging of deep waters is evidenced by the two distinct inverse correlations between AOU and eHS in the Atlantic (Figure 7, eHS = −0.15 AOU + 36.6 ± 1.9 µg eq SRFA, r^2 = 0.44 n = 48) and in the Western Mediterranean sector (eHS = −0.47 ± 0.04 AOU + 59.3 ± 2.1 µg eq SRFA, r^2 = 0.77 n = 57). A multiple regression analysis involving eHS, AOU and two conservative independent variables (absolute salinity and potential temperature) then allowed to correct the slope (ΔeHS/ΔAOU) for the effects of lateral mixing. This led to corrected values of 0.18 and 0.35 µg eq SRFA/µM O2 in the Atlantic and the Mediterranean sector, respectively. Degradation of eHS in the Mediterranean sector could have been induced by an enhanced respiration rate of DOC (Christensen et al., 1989) resulting from the very low vertical flux of biogenic particles in this domain (Speicher et al., 2006), which may not be sufficient to sustain their bacterial growth (Lefevre et al., 1996).

Based on the Mediterranean AOU-eHS correlation, and assuming that eHS oxidation is the only sink, we estimated the residence time of eHS in the intermediate Mediterranean Western reservoir (200–600 m), mostly composed of LIW (28.95 $< \sigma_\Theta <$ 29.10 kg/m^3). In the Sicily Channel, the LIW enters the Western Basin at 1.1 Sverdrup (Astraldi et al., 1999) with an AOU of ~58 µM. At the Strait of Gibraltar, the MOW has an AOU signature of ~97 µM meaning that a minimum of ~39 µM of O_2 was consumed in the interior of the Western basin. Then the oxygen utilization rate (OUR) can be estimated at ~4 µM O_2/year following (2), using the residence time of water in the intermediate layer estimated by Dulaquais et al. (2017) as 9.8 years. When combined with the ΔeHS/ΔAOU slope, we estimated an eHS degradation rate (HDR) of 1.4 µg/L of eHS per year according to equation (3). Finally, considering the mean concentration of eHS in the LIW (~25 µg/L) the residence time of eHS (τ_{HS}) can be estimated to ~18 years using equation (4). This turnover time of eHS with respect to microbial degradation is probably overestimated because it only considers one sink; however, our estimation provides a turnover time of the same order as those reported for SLDOC (Hansell & Carlson, 2014). Based on the distribution of eHS, their apparent degradation in the deep sea and their short residence time in the Mediterranean Sea, we suggest classifying the Mediterranean eHS as SLDOC rather than RDOC.

$$\text{Oxygen Utilization Rate}\left(\text{OUR in } \mu\text{mol O2 L}^{-1}\text{ yr}^{-1}\right) = \frac{\text{AOU}_{SG} - \text{AOU}_{SC}}{\tau_{LIW}} \quad (2)$$

$$\text{eHS Degradation Rate}\left(\text{HDR in } \mu\text{g eHS L}^{-1}\text{ yr}^{-1}\right) = \left|\frac{\Delta\text{eHS}}{\Delta\text{AOU}}\right| \times \text{OUR} \quad (3)$$

$$\tau_{eHS}\left(\text{yr}^{-1}\right) = \frac{[\text{eHS}]_{LIW}}{\text{HDR}} \quad (4)$$

With AOU_{SG} and AOU_{SC} the apparent oxygen utilization measured in the LIW ($28.95 < \sigma_\Theta < 29.10$ kg/m^3) at the Strait of Gibraltar (58 μM) and the Sicily Channel (39 μM) respectively, τ_{LIW} the residence time of LIW in the western Mediterranean Basin (Dulaquais et al., 2017); $[eHS]_{LIW}$ is the mean concentration of eHS recorded in the LIW (25 μg/L), and ΔeHS/ΔAOU is the multiple linear regression coefficient of the eHS-AOU correlation.

Interestingly in the WMDW (<1250 m), eHS did not correlate to AOU (Figure 7, black dots) and kept constant concentrations (15 ± 2 μg/L). This absence of a correlation in this water mass might be interpreted as the occurrence of a specific pool of eHS truly recalcitrant. As described in section 3 the WMDW is formed in winter by deep convection of surface and intermediate waters in the Gulf of Lion. This dissolved organic matter could contain a significant part of terrestrial DOC and terrestrial humics due to the direct proximity of the Rhone River (Figure 1), a major source of DOC to the Mediterranean Sea (Sempéré et al., 2000). It is possible that the eHS of this water mass are partially of terrestrial origin. In this scenario, two pools of eHS with different quality coexist in the deep Western Mediterranean Sea:(i) the marine eHS, produced at the surface and entrained by the Mediterranean circulation in the intermediate waters, which are available for heterotrophic bacterial metabolism; and (ii) A terrestrial pool fully of humics carried by Northern Rivers and trapped in the deep sea by WDMW convection, which is truly recalcitrant.

Another hypothesis to explain the constant eHS concentrations in the WMDW could be the limited degradation of eHS below 1,000 m. The low abundance of heterotrophic bacteria in the bathypelagic Western Mediterranean Sea (Tanaka & Rassoulzadegan, 2002) could lead to limited respiration of eHS in the bathypelagic layer. In this condition input and degradation of eHS are balanced and the only sinks of eHS from the largest depth would be the upwelling of deep waters to the mesopelagic layer as well as their removal from the water column by adsorption/coagulation onto sinking particles.

4.4. Connections Between eHS and Fe Chemistry

Humics have been identified as an important class of iron binding ligands (L_{Fe}) especially in coastal areas and close to shelves (Abualhaija et al., 2015; Bundy et al., 2015; Laglera & van den Berg, 2009; Mahmood et al., 2015; Muller & Cuscov, 2017). Because the Mediterranean Sea is surrounded by continents and the main Mediterranean rivers are located in the Western Basin, HS could play an important role in the complexation of DFe in this basin. Based on the relatively low conditional stability constants ($10.6 \pm 0.2 \leq \log K'_{FeHS} \leq 11.1 \pm 0.2$) of humic-type ligands for iron complexation determined by Laglera and van den Berg (2009) using SRFA and SRHA as model, humics are generally considered as a weaker class of ligands (L_2) than siderophores (L_1, $\log K'_{FeL1} > 12$; Buck et al., 2016; Rijkenberg et al., 2008). Then humics, assumed to be relatively weak, become important for the biogeochemical cycle of Fe when the relatively stronger ligands are saturated. Gerringa et al. (2017) have reported iron binding ligand concentrations (L_{Fe}) along the section. According to the method used in their study, the contribution of humic substances to the total ligand pool might be underestimated, as acknowledged by the authors. Nevertheless, Slagter et al. (2017) showed that L_{Fe} concentrations obtained with this method increases with humic concentrations and in the following paragraphs we have considered that L_{Fe} concentrations determined by Gerringa et al. (2017; noted L_{FeTAC} hereafter) included at least part of the complexing capacity of humics. This assumption was further supported by the conditional stability constant of iron binding ligands determined ($11.5 \leq \log K'L_{FeTAC} \leq 12.1$) by Gerringa et al. (2017), which falls into the range of L_2 attributed to iron humic-like complexes ($10.6 \pm 0.2 \leq \log K'_{FeL2} \leq 12.5 \pm 0.2$) in several environmental studies (Abualhaija et al., 2015; Batchelli et al., 2010; Bundy et al., 2014, 2015; Mahmood et al., 2015: Muller & Cuscov, 2017). In the Atlantic sector, the vertical distribution DFe and eHS were opposite (Figure 8c) and the absence of a clear correlation between both variables suggest restricted interactions between eHS and DFe cycles in this sector. In contrast, similar distributions between DFe and eHS were observed in the Mediterranean Sea as exemplified in

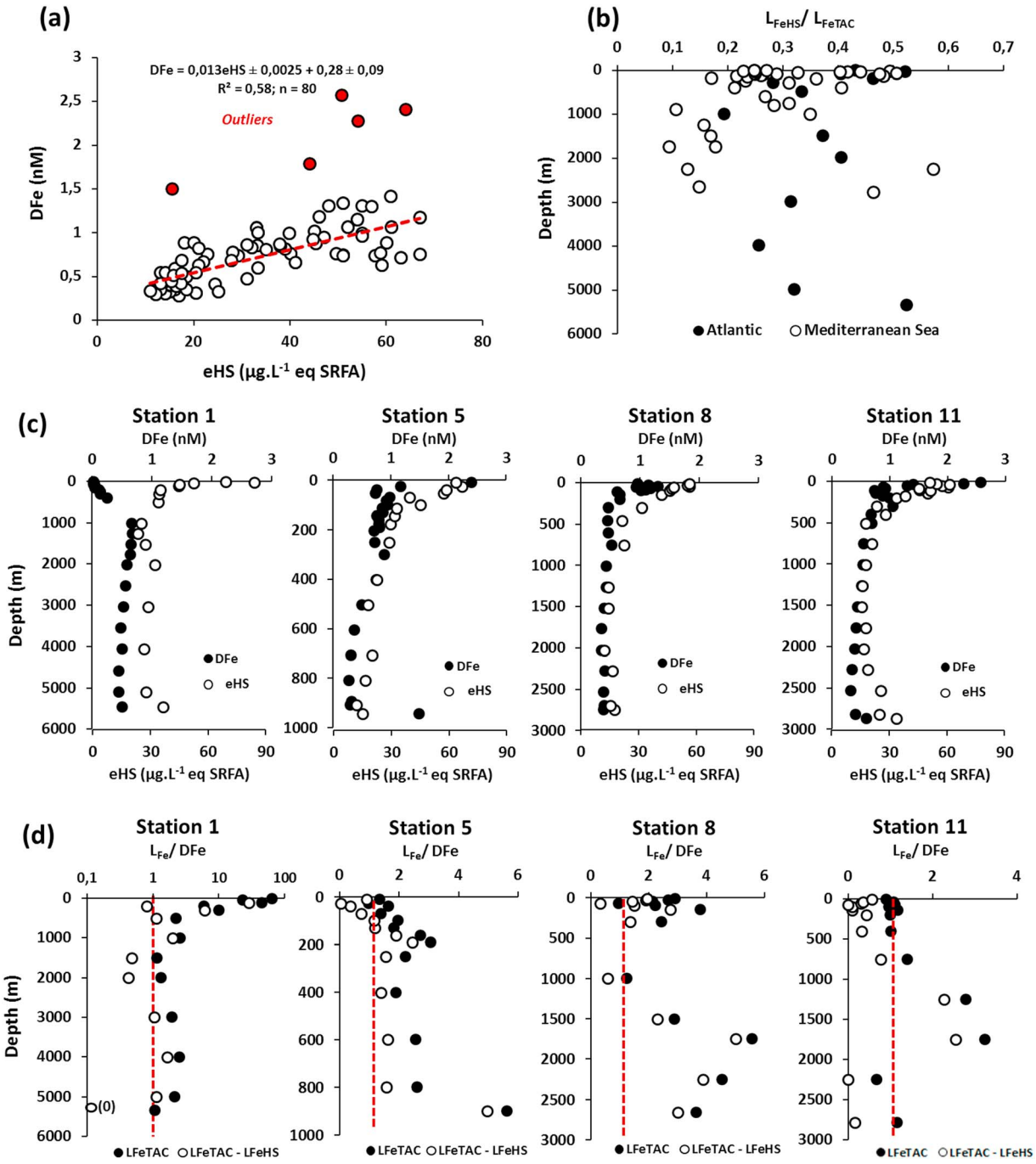

Figure 8. (a) Correlation between dissolved iron (DFe) and electroactive humic-like substances (eHS) for Mediterranean stations. Outliers (red dots) were excluded from the regression. (b) Vertical distribution of the relative contribution of eHS (L_{FeHS}) to the L_{Fe} in the Atlantic (black dots) and in the Mediterranean sector (white dots). Vertical distributions at station 1 in the Atlantic sector and stations 5, 8, and 11 in the Mediterranean sector of (c) dissolved iron (black dots) and of electroactive humic-like substances (eHS, circles) and (d) iron ligands (L_{Fe}) to DFe ratios (L_{Fe}/DFe) when total ligand concentration measured by Gerringa et al. (2017) is considered (L_{FeTAC}, black dots) and when the complexing capacity of HS is removed ($L_{FeTAC} - L_{FeHS}$, open circles). The dashed red line indicates the saturation ratio of 1.

Figure 8c for stations 5, 8, and 11. Moreover, DFe and eHS concentrations followed a significant correlation when all Mediterranean data are considered ($r^2 > 0.58$; p value $< 10^{-16}$ $n = 80$), with a positive DFe/eHS slope of 13 ± 2.5 nmol DFe/mg eq SRFA (Figure 8a). Interestingly this ratio falls into the range of the complexing capacity of SRFA (16.7 ± 2 nmol Fe/mg SRFA) determined by Laglera and van den Berg (2009) when uncertainties are considered. These observations indicate connections between the Mediterranean

cycles of iron and humics through the complexation of DFe by eHS. Based on the complexing capacity of eHS for iron (noted L_{FeHS} hereafter, with L_{FeHS} = [eHS] × 0.0167, after Laglera & van den Berg, 2009), we estimated the contribution of eHS to the total iron binding ligand pool (L_{FeHS}/L_{FeTAC}) along the water column (Figure 8b). Our estimation indicates that eHS could account for 30 ± 12% (n = 51) of the total ligand pool in both the Atlantic and Mediterranean Sea. The eHS contribution to the iron binding ligand pool could be particularly high (up to 50%) in the surface waters of the Mediterranean Sea (Figure 8b).

In order to understand the role of eHS in the Fe chemistry, we then attempted to determine at which depths eHS is important for buffering DFe against hydrolysis and subsequent precipitation. For this purpose, we compared the vertical distribution of the iron binding ligand to DFe ratios (L_{Fe}/DFe) along the water column (Figure 8d) when the complexing capacity of eHS is included in (i) or excluded from (ii) L_{Fe}:

1. The ligand concentrations are those determined by Gerringa et al. (2017) and include at least part of eHS, $L_{Fe} = L_{FeTAC}$.
2. The complexing capacity of eHS is subtracted from the ligands concentrations determined by Gerringa et al. (2017) $L_{Fe} = L_{FeTAC} - L_{FeHS}$ with $L_{Fe\text{-}HS}$ = [eHS] × 0.0167 after Laglera and van den Berg (2009)

In the Atlantic when total iron binding ligands concentrations are considered (situation (i), Figure 8d, black dots), L_{Fe} largely exceeded DFe in the surface waters and decreased with depth to L_{Fe}/DFe values between 1.1 and 2 below 1,500 m. Differently in the surface waters of the Mediterranean Sea, L_{Fe} were close to be saturated at some depths and even below DFe in few samples (e.g., 27 m at station 5, 71 m at station 8, and 100 m at station 11). This suggest that Fe is almost fully complexed (>99%) by L_{Fe} in both basins but also that Fe reactivity could be more impacted by L_{Fe} biogeochemistry in the deep Atlantic and in the surface Mediterranean Sea due to the low excess of L_{Fe}. At these depths, a slight decrease of L_{Fe} (e.g., by mineralization) would lead to iron scavenging by marine snow or by sinking dust as described by Gerringa et al. (2017). When the complexing capacity of eHS is now substracted from L_{Fe} (situation (ii) Figure 8d white dots), it clearly reveals where eHS are involved or not in the complexation of Fe. Without eHS complexing capacity, L_{Fe} would still be far from saturation (L_{Fe}/DFe > 10) in the surface Atlantic, indicating occurrence of unsaturated strong iron binding ligands in these waters. Differently, without eHS contribution, L_{Fe} would be saturated in large part of the water column in both Atlantic (1,500–3,000 m) and Mediterranean basins (upper 500 m) and more prone to scavenging processes at these depths. In other words, at these depths eHS apparently keep DFe in solution and DFe chemistry could be tightly linked to eHS biogeochemistry. Despite uncertainties resulting from our method which does not quantify the Fe-eHS complexes, and despite the competition between trace elements for complexation by humics (e.g., copper, Abualhaija et al., 2015; Whitby & van den Berg, 2015), these estimations imply that humics are involved in the speciation of Fe and thus affect its biogeochemistry in the deep Atlantic as well as the surface and the upper mesopelagic waters of the Mediterranean Sea.

Connecting these results to the eHS cycle allows an interpretation of the sharp DFe decrease in the upper 500 m of the Mediterranean water column (Figure 8c). In this domain, the large input of DFe induced by dust dissolution lead to high DFe concentrations (Gerringa et al., 2017) that can saturate strong iron binding ligands (Figure 8d). Together with high eHS concentrations (biologically mediated), it can lead to the formation of Fe-eHS complexes. As seen in the previous section (e.g., section 4.3), eHS are degraded by mineralization in the mesopelagic waters (Figure 7b). The degradation of eHS probably releases DFe in an inorganic form, which can be removed from the dissolved fraction by scavenging on sinking dust (Gerringa et al., 2017) and by precipitation as iron oxyhydroxides, in absence of empty sites of strong Fe ligands at these depths. All these processes design an "iron-humic shuttle" between the surface and the deep Mediterranean Sea. In contrast, in the Eastern Atlantic and in the deep Mediterranean Sea, strong iron-binding ligands usually exceed DFe (Figure 8d); thus, the role of eHS could be limited to increase the iron solubility at depths where the strongest ligands are (nearly) saturated.

5. Conclusion

This study provides the first comprehensive and semi quantitative data set of eHS in the Eastern Atlantic Ocean and in the Western Mediterranean Sea. We identified key processes in the marine biogeochemical cycle of eHS and suggest classifying eHS as SLDOC rather than RDOC. The vertical distribution with high

surface concentrations decreasing with depth was explained by two main processes: biological production in surface waters and microbial degradation in the mesopelagic layer. The biological mediated production suggested by a eHS-Chl *a* correlation seemed to be the main source of eHS in open sea; however, rain and riverine inputs could impact surface eHS concentrations locally. From the analysis of the significant eHS-AOU correlations, we estimated that the mesopelagic stock of eHS could be degraded by heterotrophic bacteria in nearly two decades which is in the same timescale as the residence time of SLDOC.

DFe and eHS showed similar distributions and a strong correlation in the Mediterranean sector. The eHS-DFe regression showed a positive slope of 13 ± 2.5 nmol DFe/mg SRFA and suggested that eHS were, at least partially, involved in the complexation of DFe. Moreover, we identified a probable connection between the biogeochemical cycles of Fe and eHS. We suggest that in surface waters of the Mediterranean Sea, relatively low concentrations of strong Fe binding ligands and high input of DFe by dust dissolution allows the chelation of Fe by eHS. Then in the mesopelagic layer, the degradation of eHS releases Fe which would be prone to scavenging by sinking dust, all creating an "iron-humic shuttle" between the upper and deep water column.

This work is a new step in our understanding of eHS biogeochemisty and raised questions about the crucial role of eHS in the Fe cycle. On the other side, it also revealed the need for additional quantitative eHS data in marine system, for robust identification of the different humic groups and for the development of intercalibration exercises between methods (fluorescent methods vs electrochemical and chromatographic methods).

Acknowledgments
All the electroactive humic-like substances concentrations used in this study can be found in the supporting information. We are indebted to the captain, officers, and crew members of the R/V *Pelagia*. We would like to warmly thank Hein de Baar for his help in organizing the cruise. We also thank NIOZ-Marine Research Facilities onshore and on board for their support. We warmly thank as well S. Ober, M. Laan, S. van Heuven, S. Asjes, and L. Wuis for providing high-quality CTD data. We thank Chiara Santinelli for communication of dissolved organic carbon data. We acknowledge X. Carton for his help in interpreting the dynamics of eddies along the section. We warmly thank J. Lepioufle for typesetting corrections. This investigation was supported by the GEOTRACES Med. &Black Seas project coordinated by Marie Boye and funded by the LABEX-MER Program of the Ministère de l'Education Nationale, de l'Enseignement Supérieur et de la Recherche. Micha Rijkenberg was supported by the Netherlands Organization for Scientific Research (NWO) project grant 822.01.015 (GEOTRACES, the biogeochemical cycles of bioessential trace metals and isotopes in the Mediterranean Sea and Black Sea). This investigation is a contribution to the international GEOTRACES program.

References

Abbt-Braun, G., & Frimmel, F. H. (2002). Setting the scene. In *Refractory organic substances in the environment* (Vol. 1, pp. 1–54).
Abualhaija, M. M., Whitby, H., & van den Berg, C. M. G. (2015). Competition between copper and iron for humic ligands in estuarine waters. *Marine Chemistry*, *172*, 46–56. https://doi.org/10.1016/j.marchem.2015.03.010
Aiken, G. R. (1985). Humic substances in soil, sediment, and water: Geochemistry, isolation, and characterization. *CU Authors Book Gallery*. *111*.
Alberts, J. J., & Takács, M. (1999). Importance of humic substances for carbon and nitrogen transport into southeastern United States estuaries. *Organic Geochemistry*, *30*(6), 385–395. https://doi.org/10.1016/S0146-6380(99)00024-8
Astraldi, M., Balopoulos, S., Candela, J., Font, J., Gacic, M., Gasparini, G. P., et al. (1999). The role of straits and channels in understanding the characteristics of Mediterranean circulation. *Progress in Oceanography*, *44*(1-3), 65–108. https://doi.org/10.1016/S0079-6611(99)00021-X
Avery, G. B., Willey, J. D., Kieber, R. J., Shank, G. C., & Whitehead, R. F. (2003). Flux and bioavailability of Cape Fear River and rainwater dissolved organic carbon to Long Bay, southeastern United States. *Global Biogeochemical Cycles*, *17*(2), 1042. https://doi.org/10.1029/2002GB001964
Batchelli, S., Muller, F. L. L., Chang, K. -C., & Lee, C.-L. (2010). Evidence for strong but dynamic iron-humic colloidal associations in humic-rich coastal waters. *Environmental Science & Technology*, *44*(22), 8485–8490. https://doi.org/10.1021/es101081c
Béthoux, J. P., Morin, P., Chaumery, C., Connan, O., Gentili, B., & Ruiz-Pino, D. (1998). Nutrients in the Mediterranean Sea, mass balance and statistical analysis of concentrations with respect to environmental change. *Marine Chemistry*, *63*(1-2), 155–169. https://doi.org/10.1016/S0304-4203(98)00059-0
Boyd, P. W., & Ellwood, M. J. (2010). The biogeochemical cycle of iron in the ocean. *Nature Geoscience*, *3*(10), 675–682. https://doi.org/10.1038/ngeo964
Boyle, E. S., Guerriero, N., Thiallet, A., Vecchio, R. D., & Blough, N. V. (2009). Optical properties of humic substances and CDOM: Relation to structure. *Environmental Science & Technology*, *43*(7), 2262–2268. https://doi.org/10.1021/es803264g
Brinkmann, T., Sartorius, D., & Frimmel, F. H. (2003). Photobleaching of humic rich dissolved organic matter. *Aquatic Sciences-Research Across Boundaries*, *65*(4), 415–424. https://doi.org/10.1007/s00027-003-0670-9
Bronk, D. A., See, J. H., Bradley, P., & Killberg, L. (2007). DON as a source of bioavailable nitrogen for phytoplankton. *Biogeosciences*, *4*(3), 283–296. https://doi.org/10.5194/bg-4-283-2007
Bryden, H. L., & Kinder, T. H. (1991). Steady two-layer exchange through the Strait of Gibraltar. *Deep Sea Research Part A. Oceanographic Research Papers*, *38*, S445–S463. https://doi.org/10.1016/S0198-0149(12)80020-3
Buck, K. N., Gerringa, L. J., & Rijkenberg, M. J. (2016). An intercomparison of dissolved iron speciation at the Bermuda Atlantic Time-series Study (BATS) site: Results from GEOTRACES Crossover Station A. *Frontiers in Marine Science*, *3*, 262.
Bundy, R. M., Abdulla, H. A., Hatcher, P. G., Biller, D. V., Buck, K. N., & Barbeau, K. A. (2015). Iron-binding ligands and humic substances in the San Francisco Bay estuary and estuarine-influenced shelf regions of coastal California. *Marine Chemistry*, *173*, 183–194. https://doi.org/10.1016/j.marchem.2014.11.005
Bundy, R. M., Biller, D. V., Buck, K. N., Bruland, K. W., & Barbeau, K. A. (2014). Distinct pools of dissolved iron-binding ligands in the surface and benthic boundary layer of the California current. *Limnology and Oceanography*, *59*(3), 769–787. https://doi.org/10.4319/lo.2014.59.3.0769
Carlson, C. A., Hansell, D. A., Nelson, N. B., Siegel, D. A., Smethie, W. M., Khatiwala, S., et al. (2010). Dissolved organic carbon export and subsequent remineralization in the mesopelagic and bathypelagic realms of the North Atlantic basin. *Deep Sea Research Part II: Topical Studies in Oceanography*, *57*(16), 1433–1445. https://doi.org/10.1016/j.dsr2.2010.02.013
Catalá, T. S., Reche, I., Ramón, C. L., López-Sanz, À., Álvarez, M., Calvo, E., & Álvarez-Salgado, X. A. (2016). Chromophoric signatures of microbial by-products in the dark ocean. *Geophysical Research Letters*, *43*, 7639–7648. https://doi.org/10.1002/2016GL069878
Chanudet, V., Filella, M., & Quentel, F. (2006). Application of a simple voltammetric method to the determination of refractory organic substances in freshwaters. *Analytica Chimica Acta*, *569*(1-2), 244–249. https://doi.org/10.1016/j.aca.2006.03.097
Chen, R. F., & Bada, J. L. (1992). The fluorescence of dissolved organic matter in seawater. *Marine Chemistry*, *37*(3–4), 191–221. https://doi.org/10.1016/0304-4203(92)90078-O
Chen, W. B., Smith, D. S., & Guéguen, C. (2013). Influence of water chemistry and dissolved organic matter (DOM) molecular size on copper and mercury binding determined by multiresponse fluorescence quenching. *Chemosphere*, *92*(4), 351–359.

Christensen, J. P., Packard, T. T., Dortch, F. Q., Minas, H. J., Gascard, J. C., Richez, C., & Garfield, P. C. (1989). Carbon oxidation in the deep Mediterranean Sea: Evidence for dissolved organic carbon source. *Global Biogeochemical Cycles*, *3*(4), 315–335. https://doi.org/10.1029/GB003i004p00315

Coates, J. D., Cole, K. A., Chakraborty, R., O'Connor, S. M., & Achenbach, L. A. (2002). Diversity and ubiquity of bacteria capable of utilizing humic substances as electron donors for anaerobic respiration. *Applied and Environmental Microbiology*, *68*(5), 2445–2452. https://doi.org/10.1128/AEM.68.5.2445-2452.2002

Coble, P. G. (1996). Characterization of marine and terrestrial DOM in seawater using excitation-emission matrix spectroscopy. *Marine Chemistry*, *51*(4), 325–346.

Coble, P. G. (2007). Marine optical biogeochemistry: The chemistry of ocean color. *Chemical Reviews*, *107*(2), 402–418. https://doi.org/10.1021/cr050350+

Cottrell, M. T., & Kirchman, D. L. (2000). Natural assemblages of marine proteobacteria and members of the Cytophaga-Flavobacter cluster consuming low-and high-molecular-weight dissolved organic matter. *Applied and Environmental Microbiology*, *66*(4), 1692–1697. https://doi.org/10.1128/AEM.66.4.1692-1697.2000

Croot, P. L., & Johansson, M. (2000). Determination of iron speciation by cathodic stripping voltammetry in seawater using the competing ligand 2-(2-Thiazolylazo)-p-cresol (TAC). *Electroanalysis*, *12*(8), 565–576. https://doi.org/10.1002/(SICI)1521-4109(200005)12:8<565::AID-ELAN565>3.0.CO;2-L

Dafner, E. V., Sempéré, R., & Bryden, H. L. (2001). Total organic carbon distribution and budget through the Strait of Gibraltar in April 1998. *Marine Chemistry*, *73*(3-4), 233–252. https://doi.org/10.1016/S0304-4203(00)00109-2

de Baar, H. J., Timmermans, K. R., Laan, P., De Porto, H. H., Ober, S., Blom, J. J., et al. (2008). Titan: A new facility for ultraclean sampling of trace elements and isotopes in the deep oceans in the international Geotraces program. *Marine Chemistry*, *111*(1), 4–21. https://doi.org/10.1016/j.marchem.2007.07.009

Dittmar, T., & Kattner, G. (2003). Recalcitrant dissolved organic matter in the ocean: Major contribution of small amphiphilics. *Marine Chemistry*, *82*(1–2), 115–123. https://doi.org/10.1016/S0304-4203(03)00068-9

Dulaquais, G., Planquette, H., L'Helguen, S., Rijkenberg, M. J., & Boye, M. (2017). The biogeochemistry of cobalt in the Mediterranean Sea. *Global Biogeochemical Cycles*, *31*, 377–399. https://doi.org/10.1002/2016GB005478

Durrieu de Madron, X., Houpert, L., Puig, P., Sanchez-Vidal, A., Testor, P., Bosse, A., et al. (2013). Interaction of dense shelf water cascading and open-sea convection in the northwestern Mediterranean during winter 2012. *Geophysical Research Letters*, *40*, 1379–1385. https://doi.org/10.1002/grl.50331

Elbaz-Poulichet, F., Morley, N. H., Beckers, J. M., & Nomerange, P. (2001). Metal fluxes through the strait of Gibraltar: The influence of the Tinto and Odiel rivers (SW Spain). *Marine Chemistry*, *73*(3-4), 193–213. https://doi.org/10.1016/S0304-4203(00)00106-7

Ertel, J. R., Hedges, J. I., Devol, A. H., Richey, J. E., & Ribeiro, M. D. N. G. (1986). Dissolved humic substances of the Amazon River system. *Limnology and Oceanography*, *31*(4), 739–754. https://doi.org/10.4319/lo.1986.31.4.0739

Filella, M. (2009). Freshwaters: Which NOM matters? *Environmental Chemistry Letters*, *7*(1), 21–35.

Filella, M. (2010). Quantifying 'humics' in freshwaters: Purpose and methods. *Chemistry and Ecology*, *26*(sup2), 177–186. https://doi.org/10.1080/02757540.2010.494159

Gerringa, L. J. A., Rijkenberg, M. J. A., Schoemann, V., Laan, P., & de Baar, H. J. W. (2015). Organic complexation of iron in the West Atlantic Ocean. *Marine Chemistry*, *177*, 434–446. https://doi.org/10.1016/j.marchem.2015.04.007

Gerringa, L. J. A., Rijkenberg, M. J. A., Thuróczy, C.-E., & Maas, L. R. M. (2014). A critical look at the calculation of the binding characteristics and concentration of iron complexing ligands in seawater with suggested improvements. *Environmental Chemistry*, *11*, 114–136.

Gerringa, L. J. A., Slagter, H. A., Bown, J., van Haren, H., Laan, P., de Baar, H. J. W., & Rijkenberg, M. J. A. (2017). Dissolved Fe and Fe-binding organic ligands in the Mediterranean Sea–GEOTRACES G04. *Marine Chemistry*, *194*, 100–113. https://doi.org/10.1016/j.marchem.2017.05.012

Gledhill, M., & Buck, K. N. (2012). The organic complexation of iron in the marine environment: A review. *Frontiers in Microbiology*, *3*, 69.

Gledhill, M., & van den Berg, C. M. G. (1994). Determination of complexation of iron (III) with natural organic complexing ligands in seawater using cathodic stripping voltammetry. *Marine Chemistry*, *47*(1), 41–54. https://doi.org/10.1016/0304-4203(94)90012-4

Hansell, D. A., & Carlson, C. A. (2014). *Biogeochemistry of Marine Dissolved Organic Matter* (2nd ed.). Elsevier Inc.

Hassler, C. S., van den Berg, C. M. G., & Boyd, P. W. (2017). Toward a regional classification to provide a more inclusive examination of the ocean biogeochemistry of iron-binding ligands. *Frontiers in Marine Science*, *4*, 19.

Heller, M. I., Gaiero, D. M., & Croot, P. L. (2013). Basin scale survey of marine humic fluorescence in the Atlantic: Relationship to iron solubility and H2O2. *Global Biogeochemical Cycles*, *27*, 88–100. https://doi.org/10.1029/2012GB004427

Hessen, D., & Tranvik, L. (Eds) (2013). *Aquatic humic substances: Ecology and biogeochemistry* (Vol. 133). Berlin: Springer Science & Business Media.

Huber, S. A., Balz, A., Abert, M., & Pronk, W. (2011). Characterisation of aquatic humic and non-humic matter with size-exclusion chromatography–organic carbon detection–organic nitrogen detection (LC-OCD-OND). *Water Research*, *45*(2), 879–885. https://doi.org/10.1016/j.watres.2010.09.023

IUPAC (1978). *Technical Reports and Recommendations. Pure & Applied Chemistry* (Vol. 50, pp. 65–73). Printed in Great Britain: Pergamon Press.

Jiao, N., Herndl, G. J., Hansell, D. A., Benner, R., Kattner, G., Wilhelm, S. W., et al. (2010). Microbial production of recalcitrant dissolved organic matter: Long-term carbon storage in the global ocean. *Nature Reviews Microbiology*, *8*(8), 593–599. https://doi.org/10.1038/nrmicro2386

Jørgensen, L., Stedmon, C. A., Kragh, T., Markager, S., Middelboe, M., & Søndergaard, M. (2011). Global trends in the fluorescence characteristics and distribution of marine dissolved organic matter. *Marine Chemistry*, *126*(1-4), 139–148. https://doi.org/10.1016/j.marchem.2011.05.002

Kieber, R. J., Hydro, L. H., & Seaton, P. J. (1997). Photooxidation of triglycerides and fatty acids in seawater: Implication toward the formation of marine humic substances. *Limnology and Oceanography*, *42*(6), 1454–1462. https://doi.org/10.4319/lo.1997.42.6.1454

Kieber, R. J., Peake, B., Willey, J. D., & Avery, G. B. (2002). Dissolved organic carbon and organic acids in coastal New Zealand rainwater. *Atmospheric Environment*, *36*(21), 3557–3563. https://doi.org/10.1016/S1352-2310(02)00273-X

Krivácsy, Z., Gelencsér, A., Kiss, G., Mészáros, E., Molnár, Á., Hoffer, A., et al. (2001). Study on the chemical character of water soluble organic compounds in fine atmospheric aerosol at the Jungfraujoch. *Journal of Atmospheric Chemistry*, *39*(3), 235–259. https://doi.org/10.1023/A:1010637003083

Laglera, L. M., Battaglia, G., & van den Berg, C. M. G. (2007). Determination of humic substances in natural waters by cathodic stripping voltammetry of their complexes with iron. *Analytica Chimica Acta*, *599*(1), 58–66. https://doi.org/10.1016/j.aca.2007.07.059

Laglera, L. M., Battaglia, G., & van den Berg, C. M. G. (2011). Effect of humic substances on the iron speciation in natural waters by CLE/CSV. *Marine Chemistry*, *127*(1-4), 134–143. https://doi.org/10.1016/j.marchem.2011.09.003

Laglera, L. M., & van den Berg, C. M. G. (2009). Evidence for geochemical control of iron by humic substances in seawater. *Limnology and Oceanography*, *54*(2), 610–619. https://doi.org/10.4319/lo.2009.54.2.0610

Lefevre, D., Denis, M., Lambert, C. E., & Miquel, J. C. (1996). Is DOC the main source of organic matter remineralization in the ocean water column? *Journal of Marine Systems*, *7*(2–4), 281–291. https://doi.org/10.1016/0924-7963(95)00003-8

Li, Y. H., & Peng, T. H. (2002). Latitudinal change of remineralization ratios in the oceans and its implication for nutrient cycles. *Global Biogeochemical Cycles*, *16*(4), 1130. https://doi.org/10.1029/2001GB001828

Liu, S., Lim, M., Fabris, R., Chow, C. W., Drikas, M., Korshin, G., & Amal, R. (2010). Multi-wavelength spectroscopic and chromatography study on the photocatalytic oxidation of natural organic matter. *Water Research*, *44*(8), 2525–2532. https://doi.org/10.1016/j.watres.2010.01.036

Liu, X., & Millero, F. J. (2002). The solubility of iron in seawater. *Marine Chemistry*, *77*(1), 43–54. https://doi.org/10.1016/S0304-4203(01)00074-3

Mahmood, A., Abualhaija, M. M., van den Berg, C. M. G., & Sander, S. G. (2015). Organic speciation of dissolved iron in estuarine and coastal waters at multiple analytical windows. *Marine Chemistry*, *177*, 706–719. https://doi.org/10.1016/j.marchem.2015.11.001

Marie, L., Pernet-Coudrier, B., Waeles, M., & Riso, R. (2017). Seasonal variation and mixing behaviour of glutathione, thioacetamide and fulvic acids in a temperate macrotidal estuary (Aulne, NW France). *Estuarine, Coastal and Shelf Science*, *184*, 177–190. https://doi.org/10.1016/j.ecss.2016.11.018

McDougall, T. J., & Barker, P. M. (2011). Getting started with TEOS-10 and the Gibbs Seawater (GSW) oceanographic toolbox. *SCOR/IAPSO WG*, *127*, 1–28.

Mercadante, L., Hansell, D., Gonnelli, M., Pitta, E., Rijkenberg, M., Vestri, S., et al. (2016). DOC and FDOM distribution in the Mediterranean Sea: Results from the MedBlack GEOTRACES cruise, 41st CIESM Congress Proceedings, 87.

MerMex group (2011). Marine ecosystems' responses to climatic and anthropogenic forcings in the Mediterranean. *Progress in Oceanography*, *91*(2), 97–166.

Millot, C. (1987). Circulation in the western Mediterranean-Sea. *Oceanologica Acta*, *10*(2), 143–149.

Millot, C., & Taupier-Letage, I. (2005). Circulation in the Mediterranean Sea. *The Mediterranean Sea*, *5*, 323–334.

Moore, C. M., Mills, M. M., Arrigo, K. R., Berman-Frank, I., Bopp, L., Boyd, P. W., et al. (2013). Processes and patterns of oceanic nutrient limitation. *Nature Geoscience*, *6*(9), 701–710. https://doi.org/10.1038/ngeo1765

Mopper, K., Zhou, X., Kieber, R. J., Kieber, D. J., Sikorski, R. J., & Jones, R. D. (1991). Photochemical degradation of dissolved organic carbon and its impact on the oceanic carbon cycle. *Nature*, *353*(6339), 60–62. https://doi.org/10.1038/353060a0

Morley, N. H., Burton, J. D., Tankere, S. P. C., & Martin, J. M. (1997). Distribution and behaviour of some dissolved trace metals in the western Mediterranean Sea. *Deep Sea Research Part II: Topical Studies in Oceanography*, *44*(3–4), 675–691. https://doi.org/10.1016/S0967-0645(96)00098-7

Muller, F. L. L., & Cuscov, M. (2017). Alteration of the copper-binding capacity of iron-rich humic colloids during transport from peatland to marine waters. *Environmental Science & Technology*, *51*(6), 3214–3222. https://doi.org/10.1021/acs.est.6b05303

Müller-Wegener, U. (1988). Interaction of humic substances with biota. In Humic substances and their role in the environment. Report of the Dahlem workshop on humic substances and their role in the environment. Wiley (pp. 179-192).

Norman, L. (2014). The role of natural organic ligands in transformations of iron chemistry in seawater and their effect on the bioavailability or iron to marine phytoplankton, PhD thesis, School of the Environment, University of Technology, Sydney.

Obernosterer, I., & Herndl, G. J. (2000). Differences in the optical and biological reactivity of the humic and nonhumic dissolved organic carbon component in two contrasting coastal marine environments. *Limnology and Oceanography*, *45*(5), 1120–1129. https://doi.org/10.4319/lo.2000.45.5.1120

Paglione, M., Kiendler-Scharr, A., Mensah, A. A., Finessi, E., Giulianelli, L., Sandrini, S., et al. (2014). Identification of humic-like substances (HULIS) in oxygenated organic aerosols using NMR and AMS factor analyses and liquid chromatographic techniques. *Atmospheric Chemistry and Physics*, *14*(1), 25–45. https://doi.org/10.5194/acp-14-25-2014

Pavlovic, J., & Hopke, P. K. (2012). Chemical nature and molecular weight distribution of the water-soluble fine and ultrafine PM fractions collected in a rural environment. *Atmospheric Environment*, *59*, 264–271. https://doi.org/10.1016/j.atmosenv.2012.04.053

Penru, Y., Simon, F. X., Guastalli, A. R., Esplugas, S., Llorens, J., & Baig, S. (2013). Characterization of natural organic matter from Mediterranean coastal seawater. *Journal of Water Supply: Research and Technology-AQUA*, *62*(1), 42–51. https://doi.org/10.2166/aqua.2013.113

Pernet-Coudrier, B., Waeles, M., Filella, M., Quentel, F., & Riso, R. D. (2013). Simple and simultaneous determination of glutathione, thioacetamide and refractory organic matter in natural waters by DP-CSV. *Science of the Total Environment*, *463*, 997–1005.

Poulin, B. A., Ryan, J. N., & Aiken, G. R. (2014). Effects of iron on optical properties of dissolved organic matter. *Environmental Science & Technology*, *48*(17), 10,098–10,106. https://doi.org/10.1021/es502670r

Prakash, A. A., & Rashid, M. A. (1968). Influence of humic substances on the growth of marine phytoplankton: Dinoflagellates. *Limnology and Oceanography*, *13*(4), 598–606. https://doi.org/10.4319/lo.1968.13.4.0598

Quentel, F., & Elleouet, C. (2001). Square-wave voltammetry of molybdenum-fulvic acid complex. *Electroanalysis*, *13*(12), 1030–1035. https://doi.org/10.1002/1521-4109(200108)13:12<1030::AID-ELAN1030>3.0.CO;2-6

Quentel, F., Elleouet, C., & Madec, C. (1992). Synergic effect of fulvic acids on the differential pulse adsorptive voltammetry of the Mo (VI)-phenanthroline complex. *Electroanalysis*, *4*(7), 707–711. https://doi.org/10.1002/elan.1140040707

Quentel, F., & Filella, M. (2008). Quantification of refractory organic substances in freshwaters: Further insight into the response of the voltammetric method. *Analytical and Bioanalytical Chemistry*, *392*(6), 1225–1230. https://doi.org/10.1007/s00216-008-2366-4

Quentel, F., Madec, C., Bihan, A. L., & Courtot-Coupez, J. (1986). Determination des Substances Humiques en Milieu Marin Par Redissolution Cathodique a L'Electrode à Goutte Pendante de Mercure. *Analytical Letters*, *19*(3–4), 325–344. https://doi.org/10.1080/00032718608064499

Quentel, F., Madec, C., & Courtot-Coupez, J. (1987). Determination of humic substances in seawater by electrochemistry (mechanisms). *Analytical Letters*, *20*(1), 47–62. https://doi.org/10.1080/00032718708082236

Ribas-Ribas, M., Gómez-Parra, A., & Forja, J. M. (2011). Air–sea CO 2 fluxes in the north-eastern shelf of the Gulf of Cádiz (Southwest Iberian Peninsula). *Marine Chemistry*, *123*(1-4), 56–66. https://doi.org/10.1016/j.marchem.2010.09.005

Rijkenberg, M. J., de Baar, H. J., Bakker, K., Gerringa, L. J., Keijzer, E., Laan, M., et al. (2015). "PRISTINE", a new high volume sampler for ultraclean sampling of trace metals and isotopes. *Marine Chemistry*, *177*, 501–509. https://doi.org/10.1016/j.marchem.2015.07.001

Rijkenberg, M. J., Middag, R., Laan, P., Gerringa, L. J., van Aken, H. M., Schoemann, V. D., et al. (2014). The distribution of dissolved iron in the West Atlantic Ocean. *PLoS One*, *9*(6), e101323. https://doi.org/10.1371/journal.pone.0101323

Rijkenberg, M. J., Powell, C. F., Dall'Osto, M., Nielsdottir, M. C., Patey, M. D., Hill, P. G., et al. (2008). Changes in iron speciation following a Saharan dust event in the tropical North Atlantic Ocean. *Marine Chemistry*, *110*(1-2), 56–67. https://doi.org/10.1016/j.marchem.2008.02.006

Rolison, J. M., Middag, R., Stirling, C. H., Rijkenberg, M. J. A., & De Baar, H. J. W. (2015). Zonal distribution of dissolved aluminium in the Mediterranean Sea. *Marine Chemistry*, *177*, 87–100. https://doi.org/10.1016/j.marchem.2015.05.001

Rosenstock, B., Zwisler, W., & Simon, M. (2005). Bacterial consumption of humic and non-humic low and high molecular weight DOM and the effect of solar irradiation on the turnover of labile DOM in the Southern Ocean. *Microbial Ecology*, *50*(1), 90–101. https://doi.org/10.1007/s00248-004-0116-5

Rue, E. L., & Bruland, K. W. (1995). Complexation of iron (III) by natural organic ligands in the central North Pacific as determined by a new competitive ligand equilibration/adsorptive cathodic stripping voltammetric method. *Marine Chemistry*, *50*(1–4), 117–138. https://doi.org/10.1016/0304-4203(95)00031-L

Salma, I., Mészáros, T., Maenhaut, W., Vass, E., & Majer, Z. (2010). Chirality and the origin of atmospheric humic-like substances. *Atmospheric Chemistry and Physics*, *10*(3), 1315–1327. https://doi.org/10.5194/acp-10-1315-2010

Santinelli, C., Gasparini, G. P., Nannicini, L., & Seritti, A. (2002). Vertical distribution of dissolved organic carbon (DOC) in the western Mediterranean Sea in relation to the hydrological characteristics. *Deep Sea Research Part I: Oceanographic Research Papers*, *49*(12), 2203–2219. https://doi.org/10.1016/S0967-0637(02)00129-2

Santinelli, C., Nannicini, L., & Seritti, A. (2010). DOC dynamics in the meso and bathypelagic layers of the Mediterranean Sea. *Deep Sea Research Part II: Topical Studies in Oceanography*, *57*(16), 1446–1459. https://doi.org/10.1016/j.dsr2.2010.02.014

Santos, P. S., Otero, M., Duarte, R. M., & Duarte, A. C. (2009). Spectroscopic characterization of dissolved organic matter isolated from rainwater. *Chemosphere*, *74*(8), 1053–1061. https://doi.org/10.1016/j.chemosphere.2008.10.061

Schlitzer, R. (2007). Ocean data view. Retrieved from http://odv.awi.de

Schneider, B., Karstensen, J., Oschlies, A., & Schlitzer, R. (2005). Model-based evaluation of methods to determine C: N and N: P regeneration ratios from dissolved nutrients. *Global Biogeochemical Cycles*, *19*, GB2009. https://doi.org/10.1029/2004GB002256

See, J. H., & Bronk, D. A. (2005). Changes in C: N ratios and chemical structures of estuarine humic substances during aging. *Marine Chemistry*, *97*(3-4), 334–346. https://doi.org/10.1016/j.marchem.2005.05.006

Sempéré, R., Charrière, B., Van Wambeke, F., & Cauwet, G. (2000). Carbon inputs of the Rhône River to the Mediterranean Sea: Biogeochemical implications. *Global Biogeochemical Cycles*, *14*(2), 669–681. https://doi.org/10.1029/1999GB900069

Shimotori, K., Omori, Y., & Hama, T. (2009). Bacterial production of marine humic-like fluorescent dissolved organic matter and its biogeochemical importance. *Aquatic Microbial Ecology*, *58*(1), 55–66. https://doi.org/10.3354/ame01350

Slagter, H. A., Reader, H. E., Rijkenberg, M. J. A., van der Loeff, M. R., de Baar, H. J. W., & Gerringa, L. J. A. (2017). Organic Fe speciation in the Eurasian Basins of the Arctic Ocean and its relation to terrestrial DOM. *Marine Chemistry*, *197*, 11–25. https://doi.org/10.1016/j.marchem.2017.10.005

Speicher, E. A., Moran, S. B., Burd, A. B., Delfanti, R., Kaberi, H., Kelly, R. P., et al. (2006). Particulate organic carbon export fluxes and size-fractionated POC/^{234}Th ratios in the Ligurian, Tyrrhenian and Aegean Seas. *Deep Sea Research Part I: Oceanographic Research Papers*, *53*(11), 1810–1830. https://doi.org/10.1016/j.dsr.2006.08.005

Stedmon, C. A., & Markager, S. (2005). Resolving the variability in dissolved organic matter fluorescence in a temperate estuary and its catchment using PARAFAC analysis. *Limnology and Oceanography*, *50*(2), 686–697. https://doi.org/10.4319/lo.2005.50.2.0686

Tagliabue, A., Bowie, A. R., Boyd, P. W., Buck, K. N., Johnson, K. S., & Saito, M. A. (2017). The integral role of iron in ocean biogeochemistry. *Nature*, *543*(7643), 51–59. https://doi.org/10.1038/nature21058

Takahashi, T., Broecker, W. S., & Langer, S. (1985). Redfield ratio based on chemical data from isopycnal surfaces. *Journal of Geophysical Research*, *90*(C4), 6907–6924. https://doi.org/10.1029/JC090iC04p06907

Tanaka, T., & Rassoulzadegan, F. (2002). Full-depth profile (0–2000m) of bacteria, heterotrophic nanoflagellates and ciliates in the NW Mediterranean Sea: Vertical partitioning of microbial trophic structures. *Deep Sea Research Part II: Topical Studies in Oceanography*, *49*(11), 2093–2107. https://doi.org/10.1016/S0967-0645(02)00029-2

Tranvik, L. J. (1993). Microbial transformation of labile dissolved organic matter into humic-like matter in seawater. *FEMS Microbiology Ecology*, *12*(3), 177–183. https://doi.org/10.1111/j.1574-6941.1993.tb00030.x

Tranvik, L. J. (1998). *Degradation of dissolved organic matter in humic waters by bacteria*, *In aquatic humic substances (pp. 259–283)*, (). Berlin Heidelberg: Springer. https://doi.org/10.1007/978-3-662-03736-2_11

Trimborn, S., Hoppe, C. J. M., Taylor, B. B., Bracher, A., & Hassler, C. (2015). Physiological characteristics of open ocean and coastal phytoplankton communities of Western Antarctic Peninsula and Drake Passage waters. *Deep Sea Res. Part I Oceanographic Research. Papers.*, *98*, 115–124. https://doi.org/10.1016/j.dsr.2014.12.010

van Aken, H. M. (2000a). The hydrography of the mid-latitude northeast Atlantic Ocean: I: The deep water masses. *Deep Sea Research Part I: Oceanographic Research Papers*, *47*(5), 757–788. https://doi.org/10.1016/S0967-0637(99)00092-8

van Aken, H. M. (2000b). The hydrography of the mid-latitude northeast Atlantic Ocean: II: The intermediate water masses. *Deep Sea Research Part I: Oceanographic Research Papers*, *47*(5), 789–824. https://doi.org/10.1016/S0967-0637(99)00112-0

van Geen, A., Boyle, E. A., & Moore, W. S. (1991). Trace metal enrichments in waters of the Gulf of Cadiz, Spain. *Geochimica et Cosmochimica Acta*, *55*(8), 2173–2191. https://doi.org/10.1016/0016-7037(91)90095-M

Waeles, M., Riso, R., Pernet-Coudrier, B., Quentel, F., Durrieu, G., & Tissot, C. (2013). Annual cycle of humic substances in a temperate estuarine system affected by agricultural practices. *Geochimica et Cosmochimica Acta*, *106*, 231–246. https://doi.org/10.1016/j.gca.2012.12.040

Whitby, H., & van den Berg, C. M. G. (2015). Evidence for copper-binding humic substances in seawater. *Marine Chemistry*, *173*, 282–290. https://doi.org/10.1016/j.marchem.2014.09.011

Willey, J. D., Kieber, R. J., Eyman, M. S., & Avery, G. B. (2000). Rainwater dissolved organic carbon: Concentrations and global flux. *Global Biogeochemical Cycles*, *14*(1), 139–148. https://doi.org/10.1029/1999GB900036

Yamashita, Y., Cory, R. M., Nishioka, J., Kuma, K., Tanoue, E., & Jaffé, R. (2010). Fluorescence characteristics of dissolved organic matter in the deep waters of the Okhotsk Sea and the northwestern North Pacific Ocean. *Deep Sea Research Part II: Topical Studies in Oceanography*, *57*(16), 1478–1485. https://doi.org/10.1016/j.dsr2.2010.02.016

Yamashita, Y., & Jaffé, R. (2008). Characterizing the interactions between trace metals and dissolved organic matter using excitation–emission matrix and parallel factor analysis. *Environmental Science & Technology*, *42*(19), 7374–7379. https://doi.org/10.1021/es801357h

Yamashita, Y., & Tanoue, E. (2008). Production of bio-refractory fluorescent dissolved organic matter in the ocean interior. *Nature Geoscience*, *1*(9), 579–582. https://doi.org/10.1038/ngeo279

Yamashita, Y., & Tanoue, E. (2009). Basin scale distribution of chromophoric dissolved organic matter in the Pacific Ocean. *Limnology and Oceanography*, *54*(2), 598–609. https://doi.org/10.4319/lo.2009.54.2.0598

Zappoli, S., Andracchio, A., Fuzzi, S., Facchini, M. C., Gelencser, A., Kiss, G., et al. (1999). Inorganic, organic and macromolecular components of fine aerosol in different areas of Europe in relation to their water solubility. *Atmospheric Environment*, *33*(17), 2733–2743. https://doi.org/10.1016/S1352-2310(98)00362-8